Zero Export Feeder Through Transactive Markets

Sivasathya Pradha Balamurugan, Dylan Cutler,
Ted Kwasnik, Tarek Elgindy, Prateek Munankarmi,
Jeff Maguire, Michael Blonsky, Shibani Ghosh,
Rohit Chintala, and Dane Christensen

National Renewable Energy Laboratory

Produced under direction of Exelon by the National Renewable Energy Laboratory (NREL) under TSA-19-01234.

NREL is a national laboratory of the U.S. Department of Energy
Office of Energy Efficiency & Renewable Energy
Operated by the Alliance for Sustainable Energy, LLC

Contract No. DE-AC36-08GO28308

Strategic Partnership Project Report
NREL/TP-5500-78673
May 2022

Zero Export Feeder Through Transactive Markets

Sivasathya Pradha Balamurugan, Dylan Cutler,
Ted Kwasnik, Tarek Elgindy, Prateek Munankarmi,
Jeff Maguire, Michael Blonsky, Shibani Ghosh,
Rohit Chintala, and Dane Christensen

National Renewable Energy Laboratory

Suggested Citation

Sivasathya Pradha Balamurugan, Dylan Cutler, Ted Kwasnik, Tarek Elgindy, Prateek Munankarmi, Jeff Maguire, Michael Blonsky, Shibani Ghosh, Rohit Chintala, and Dane Christensen. 2022. *Zero Export Feeder Through Transactive Markets*. Golden, CO: National Renewable Energy Laboratory. NREL/TP-5500-78673. https://www.nrel.gov/docs/fy22osti/78673.pdf.

Strategic Partnership Project Report
NREL/TP-5500-78673
May 2022

National Renewable Energy Laboratory
15013 Denver West Parkway
Golden, CO 80401
303-275-3000 • www.nrel.gov

NOTICE

This work was authored by the National Renewable Energy Laboratory, operated by Alliance for Sustainable Energy, LLC, for the U.S. Department of Energy (DOE) under Contract No. DE-AC36-08GO28308. Support for the work was also provided by Exelon under TSA-19-01234. The views expressed in the article do not necessarily represent the views of the DOE or the U.S. Government. The U.S. Government retains and the publisher, by accepting the article for publication, acknowledges that the U.S. Government retains a nonexclusive, paid-up, irrevocable, worldwide license to publish or reproduce the published form of this work, or allow others to do so, for U.S. Government purposes.

Cover Photos by Dennis Schroeder: (clockwise, left to right) NREL 51934, NREL 45897, NREL 42160, NREL 45891, NREL 48097, NREL 46526.

Acknowledgments

The authors gratefully acknowledge Philip Nevels, Kristen Brown and Theresa Christian at Exelon, and Sam Hartnett, Micha Roon, and Adam Nagy at Energy Web Foundation for their contributions to this report. Amrita Pulidindi, Robert S. Stewart, Steve Steffel, Abdul Razzaq, and Qin Zhang from Pepco provided valuable data and expertise.

Special thanks to Carlo Bianchi of the National Renewable Energy Laboratory.

List of Acronyms

BAU	business as usual
DEW	Distributed Engineering Workstation
DID	Decentralized Identifier
DiTTo	Distribution Transformation Tool
ERCOT	Electric Reliability Council of Texas
EW-DOS	Energy Web Decentralized Operating System
EWF	Energy Web Foundation
EWC	Energy Web Chain
HELICS	Hierarchical Engine for Large-scale Infrastructure Co-Simulation
HEMS	home energy management system
HVAC	heating, ventilation, and air conditioning
LMP	locational marginal pricing
NEM	net energy metering
NREL	National Renewable Energy Laboratory
OCHRE	Object-oriented, Controllable, High-resolution Residential Energy
p.u.	per unit
PUMA	public use microdata area
PV	photovoltaic
RC	resistor-capacitor
SMARTER	Simple Multi-Attribute Rating Technique Exploiting Ranks
SOC	state of charge
TOU	time of use

Executive Summary

This project is aimed at creating a transactive energy market to address the challenges faced by utility providers when increasing distributed energy resource (DER) adoption in their service area. One major challenge is mitigating export back to the grid during times of excess production. The transactive energy market operates at the distribution level and balances the supply and demand on the feeder, thus maintaining a zero-energy export at the primary feeder head. The market participants in this case are the residential customers on the feeder, who bid into the market. Building controls are then optimized based on the settled price. Market performance was demonstrated in this study by simulating different levels of DER penetration on a selected Pepco feeder. The feeder successfully achieved a zero export while providing cost-effective electricity to the participants, demonstrating that this market design can enable high DER penetration on existing feeders.

Table of Contents

List of Figures

List of Tables

1 Introduction

With the adoption of distributed energy resources (DER) increasing in recent years and projected to continue, distribution utilities are assessing new ways to facilitate these installations, as they bring some unique challenges. Utilities want to support their customers by allowing them to install DER in their buildings, yet they need to manage infrastructure costs that may be required to support very high-penetration DER. Additional challenges arise around managing the operation of thousands (potentially hundreds of thousands) of installed DER. As DER adoption grows it will be difficult for a single entity like a utility to directly control all the DER on the feeder. It is also expensive to make significant infrastructure upgrades, affecting both the utility and the consumer. Furthermore, increasing DER can cause physical disruptions to the feeder; for example, excess production in buildings exported back into the feeder can cause voltage issues. Such disruptions can be a hindrance to providing reliable electricity to customers.

In this project, we aim to show that these challenges may be mitigated through the application of transactive energy markets. We implement a transactive energy market designed to ensure zero energy export at the feeder head. While the exact requirement of “zero export” may change depending on utility infrastructure and needs, this project aims to generally show that appropriate market application can achieve utility operational goals. The requirements for this distribution-level market were that it (1) be scalable to enable increasing adoption, (2) provide a cost-effective and secure solution that does not require active customer engagement, and (3) be price-driven, without need for direct control infrastructure connecting to all the DER assets. We have implemented the market using blockchain technology as it has features that enable secure tracking of market participants’ identities and secure logging of market transactions. To design and implement such a market, we needed utility operations experts to provide a business context and identify inherent challenges, and market design and software experts to enable the implementation and operation of this market structure. This led to a close collaborative partnership between Exelon utilities, the National Renewable Energy Laboratory (NREL), and the Energy Web Foundation (EWF), as shown in Figure 1.

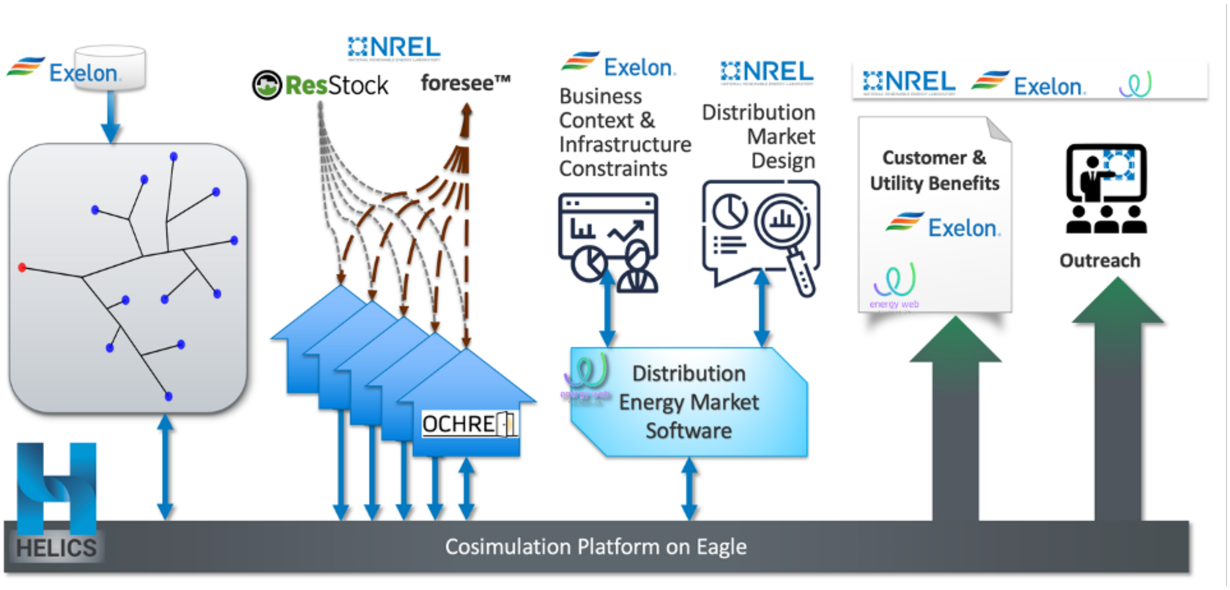

Figure 1. Summary diagram of the simulation environment implemented to test market functionality. Key players and their roles are also shown.

The transactive energy market enables zero export on the primary feeder head by balancing supply and demand at the distribution level. The market does not directly control the DER but allows home energy management systems (HEMS) to optimize for the individual home, giving the customer complete control of the DER and the loads. The HEMS submits bids on behalf of the customer and those are either approved or denied by the market based on settled price. This hands-off approach simplifies utility DER management while increasing customer satisfaction. To evaluate the performance of the transactive market, we performed a co-simulation of a representative distribution feeder, associated buildings, and the market on a Pepco feeder in the Washington, D.C. area. This allows us to simulate the system without going through the full hardware installation process and enables rapid exploration of different scenarios (e.g., increased DER penetration). By simulating scenarios with different levels of DER penetration with and without the market, we are able to evaluate the effectiveness of the market.

2 Modeling

2.1 Feeder Modeling

A distribution feeder consists of all the electrical components which connect a substation to individual customers. These include overhead and underground lines, transformers, capacitors, regulators as well as the connected loads. While most electrical distribution models only consider the primary (medium voltage) network, in this study we also consider secondary (low voltage) networks, which contain the lines connecting transformers to individual customers. Modeling the secondaries are of particular significance in this study due to the high precision of load data and its interaction with the grid through the transactive energy market.

In this study, we used a Pepco feeder located in Washington, D.C. We used primary feeder data from Exelon and data supplied from EDD under a nondisclosure agreement to model the secondaries. A mapping of transformers between these two data sets was performed to identify points of coupling between the primary and secondary models.

The Distribution Transformation Tool (DiTTo),[1] developed at NREL, was utilized to process all the distribution data for the feeder. DiTTo is a many-to-many conversion tool which allows users to ingest data from one source, apply modifications as required, and then export it to the same or different data formats. To parse and manipulate the data, DiTTo was integrated into a Python workflow consisting of several steps:

1. DiTTo was used to read the primary and secondary model data from the native Distributed Engineering Workstation (DEW) format.
2. DiTTo algorithms were used to join the two data sets into one model by identifying common transformer connection points.
3. The DiTTo validation module was used to identify any malformed data such as loops on the secondary networks or duplicate connection points for secondaries.
4. A separate Python routine was applied to clean data issues identified by DiTTo, to produce a radial network with correct attachment of secondaries.
5. A separate Python routine was used to identify the locations of loads and then apply DiTTo subroutines to attach them to the correct secondary.
6. DiTTo was used to attach the timeseries profiles provided from Advanced Metering Infrastructure data to the loads on the feeder.
7. DiTTo was used to write the output of the combined and cleaned model to OpenDSS.
8. The OpenDSSDirect Python module was used to run power flow simulations using the generated model to guarantee that load voltages were within desired bounds on feeder.

After developing and implementing the methodology described above, the OpenDSS model was integrated into the co-simulation framework and connected to the other modeling components.

2.2 Building Energy Modeling

To simulate reasonable behavior for the power consumption of each home, building energy models of different homes on this feeder were created. ResStock, a tool for national scale analysis of the residential housing stock, was used to determine the characteristics of the building energy models for this study (Wilson et al. 2017). ResStock contains probability distributions for all the characteristics of the housing stock across the entire United States and contains a workflow for modeling the stock (or any subset) in EnergyPlus®, the U.S. Department of Energy's flagship building energy modeling tool (U.S. Department of Energy 2021). For this study, ResStock was sampled for the public use microdata area (PUMA) in which this feeder is located. This sampling process looks at a wide variety of data sources to come up with a number

---

[1] https://github.com/NREL/ditto/

of archetypal building energy models that have the characteristics (e.g., wall insulation or heating, ventilation, and air conditioning [HVAC] efficiency) as the housing stock in this community, using any known housing characteristics of the PUMA (e.g., building vintage) replacing the ResStock defaults as appropriate. ResStock sampling was performed for more than 500 homes in this community, from which 50 unique building energy models were created. This down-selection greatly reduced the complexity of modeling the entire community while still preserving the same average and standard deviation in power consumption as the larger stock. Some high-level characteristics of the housing stock are provided in Figure 2.

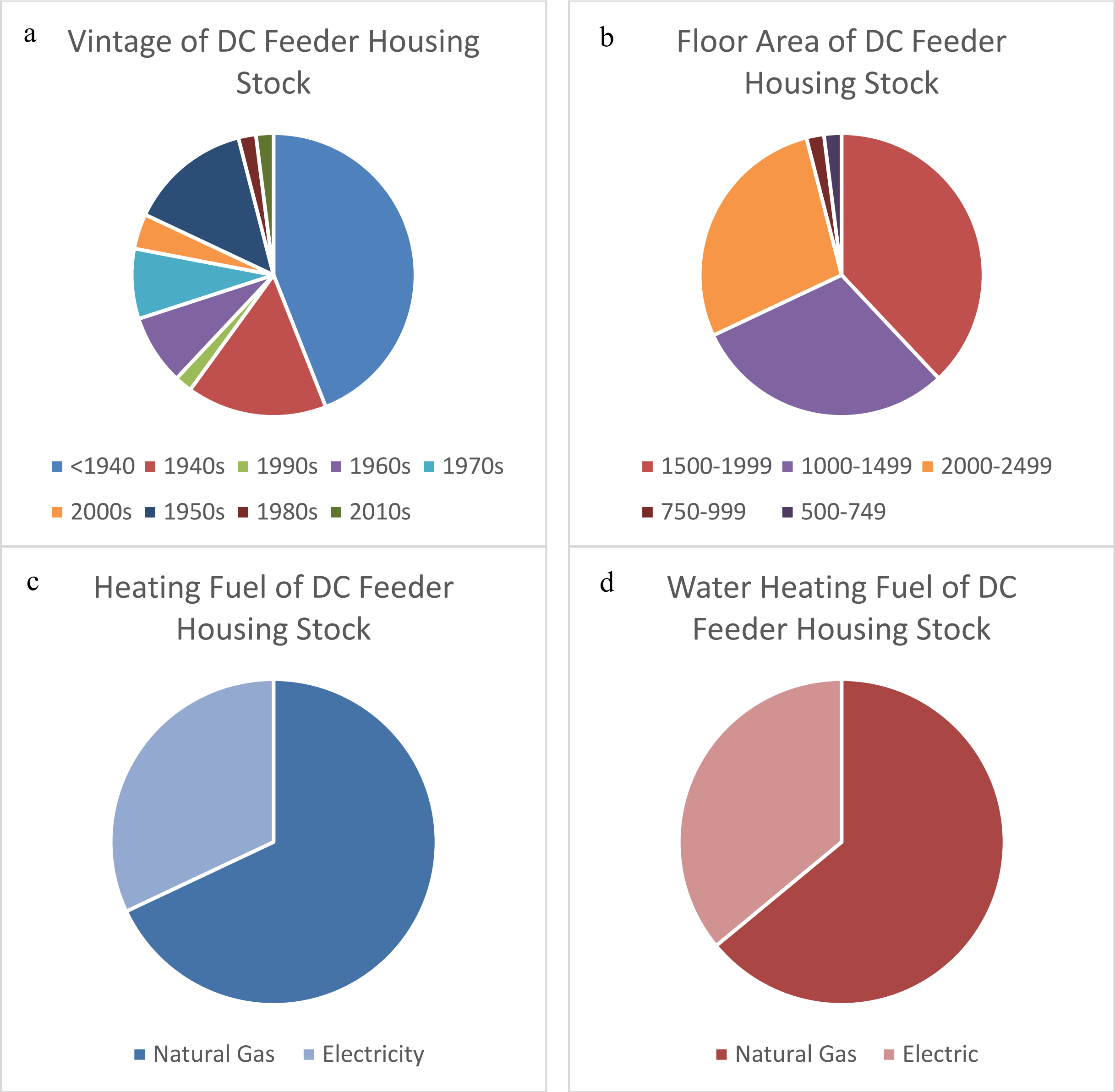

Figure 2. Key characteristics of the single-family housing stock at the feeder location, including (a) building vintage, (b) building square footage, (c) heating fuel, and (d) water heating fuel.

While ResStock was used to determine the housing characteristics, the actual building energy models were created using the Object-oriented, Controllable, High-resolution Residential Energy (OCHRE) model. OCHRE^{TM} is a new building energy modeling tool developed at NREL designed to model realistic physics and power consumption of homes specifically for co-simulation studies such as this one (Blonsky et al. 2021). OCHRE uses a white box, resistor-capacitor (RC)-based modeling approach to capture the physics of heat transfer through the building envelope as well as realistic models of the HVAC and water heater based on the approach used in EnergyPlus. It is capable of receiving control signals for the HVAC and water heater and reporting the state of each device to an external HEMS. OCHRE includes the capability to model the voltage-dependent nature of home power consumption through integrated ZIP models as well as several DER models, including solar photovoltaic (PV), home batteries, and electric vehicles. The RC network approach used in OCHRE is shown in Figure 3.

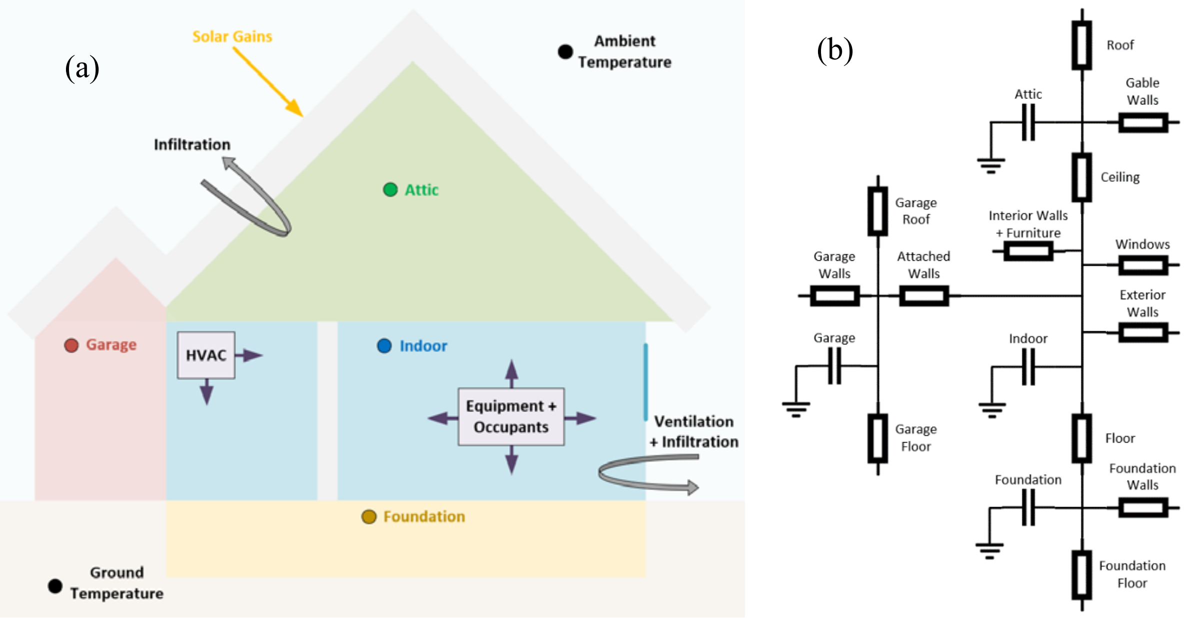

Figure 3. (a) Schematic representation of the building and (b) corresponding RC circuit used in OCHRE. Each block in (b) is made up of multiple resistors and capacitors as shown in Figure 4.

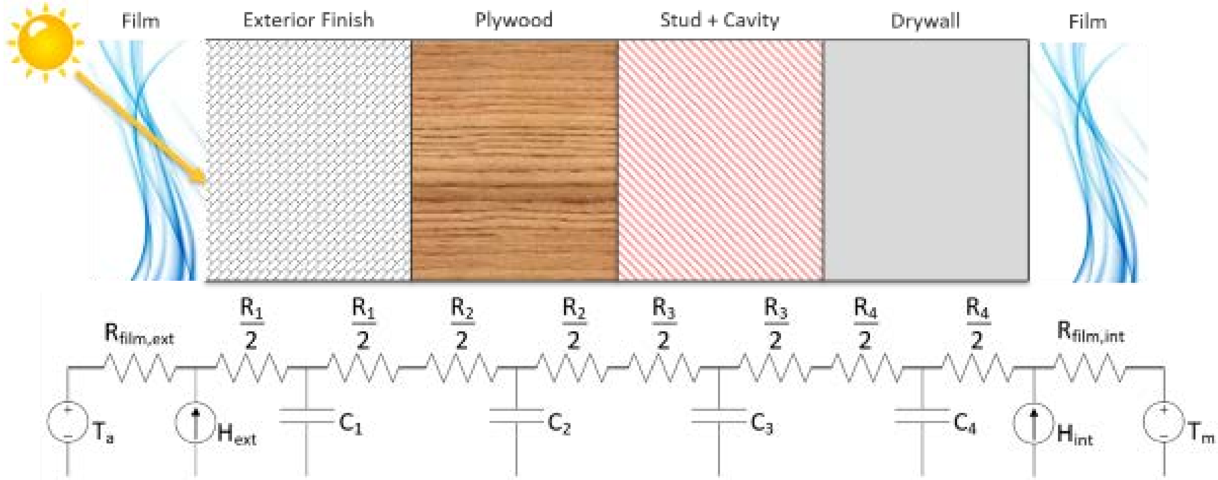

Figure 4. RC representation of a wall in OCHRE. All surfaces are treated in a similar fashion, with each material making up a single capacitor with half of the thermal resistance of the material on either side. Additional resistors are used to capture the film resistance on the sides of the material.

Each of the ResStock archetypes had a corresponding OCHRE model created, which was then compared to the corresponding EnergyPlus model. While not every home was a perfect match, on average there is a 3% difference in the electricity consumption of the building stock in EnergyPlus and OCHRE. There are some known differences between the two approaches, particularly when simulating HVAC, as EnergyPlus takes a part-load approach to perfectly maintain setpoint while OCHRE models on/off thermostat behavior with a dead band. When comparing the annual electricity consumption of the stock model to the Advanced Metering Infrastructure data for these homes, the models predict about 20% more electricity consumption than the actual measured data. However, there is some amount of PV installed in the actual homes which was not included in the housing stock model. That, along with differences in behavior (e.g., higher miscellaneous electric loads or different setpoints) likely explains the discrepancy.

3 Transactive Energy Market

3.1 Market Design

The guiding principles of the market design were as follows:

1) Achieve zero export at the feeder head over a 15-minute window

2) Deliver this functionality with a price-driven market approach, avoiding direct control of the associated DER

3) Ensure equitable distribution of market benefits (i.e., not preferentially benefiting those with solar PV or other assets).

The basis for the market is derived from the design of the wholesale electricity markets that are predominant throughout the deregulated markets of the United States. These are generally designed as a double-blind auction with equilibrium settlement that establishes the price for all participants (i.e., pay as settled, not pay as bid) (Morey 2001). These markets typically have two primary stages: a day-ahead market that is financially but not physically binding, and a real-time market that aims to resolve load and demand imbalances that materialize between the day-ahead horizon and the real-time operating horizon.

We follow a similar approach in the market design for this project. We implement both a day-ahead and real-time market and settle the markets using a double-blind auction. The double-blind auction approach is modified for this project in two primary ways: (1) we incorporate a ceiling and a floor in the market to enable cost recovery for the utility and avoid cost increases for the market participants, and (2) we include a 'surplus pricing' mechanism in the real-time market.

The market floor and ceiling bound the range within which the market can settle during each timestep of the day-ahead market. This concept is based on a previous market design by the project team (Cutler et al. 2020), though that market design only included day-ahead (not real-time operations). The market floor is set by the wholesale locational marginal pricing (LMP) at the transmission node that serves the feeder that we are evaluating. This establishes a floor to the market that is equivalent to the price that the utility would pay to procure the electricity to serve the feeder load. We then establish the ceiling of the market by calculating a 'retail adder' factor that scales up the time-varying LMP signal that sets the floor. This retail adder is calculated such that it achieves equivalent cost recovery as the prevailing utility tariff for the residential customers on the feeder (this is a residential-focused transactive market). We calculate the revenue that the utility would receive for the feeder load under the prevailing residential tariff,[2] and then calculate a scaling factor that, multiplied against the LMP for each hour year, would result in that same revenue while billing at a time-varying price.

The surplus pricing mechanism was developed specifically for the goal of zero export at the feeder head and is loosely based on the scarcity pricing mechanism that has been implemented in the Electric Reliability Council of Texas (ERCOT) energy only market.[3] The scarcity pricing in ERCOT is implemented through an Operating Reserve Demand Curve (ORDC) which essentially increases the real-time price as reserves begin to fall to a critical level and caps the price at a market ceiling established as the value of lost load. In this market design, we flip that concept on its head and establish a scarcity pricing mechanism that modifies the real-time price when the ratio of demand to supply falls below an established level. Surplus pricing reduces the settled price from the day-ahead to encourage more demand to enter the market and higher priced supply to remove bids. Expected surplus pricing is communicated to the market participants based on the cleared supply/demand quantities in the day-ahead market, allowing participants to modify bids and offers moving into real-time. If surplus persists into the real-time clearing, it modifies the settled price and can result in reduced cost for demand and value for any supply in the system.

The following section, Market Implementation, covers the details of the market operations described here.

---

[2] https://www.pepco.com/MyAccount/MyBillUsage/Documents/Updated%20060120%20-%20R.pdf

[3] https://cms.ferc.gov/sites/default/files/2020-05/20160629114652-3%2520-%2520FERC2016_Scarcity%2520Pricing_ERCOT_Resmi%2520Surendran.pdf

3.2 Market Implementation

The market agent manages day-ahead and real-time market solvers, as well as communication with the HEMS federates and the blockchain as needed. The HEMS agent which interacts with the market agent have been designed to optimize energy use on a sliding eight-hour forecasting window.

3.2.1 Day-Ahead Market Solver

In this simulation, the duration of each day-ahead market is 24 hours (from 12 a.m. to 11:59 p.m.), and the market is settled in 15-minute periods. The day-ahead market solver receives bids prior to the start of each day at a time that allows HEMS solvers to have sufficient foresight into next day's settled day-ahead prices. For example, if the HEMS are expected to submit 8 hours of forecasted real-time bids, then the day-ahead market will be resolved at 4 p.m. on the previous day. This scheme ensures that at 5 p.m. the settled day-ahead bids for the upcoming 12 a.m. to 1 a.m. settlement periods will be known to the HEMS as it constructs its forecasts.

The day-ahead market is instantiated with advance knowledge of uncontrollable loads (commercial loads and any non-participant's residential loads), as well as floor and ceiling prices, for all settlement periods. Note that floor prices are tied to established wholesale rates. Ceiling prices for the day-ahead market are bound to a scaled wholesale rate that over the course of a year would generate as much revenue as the prevailing residential electric tariff for the utility. In this simulation, cost recovery was referenced to a simplified Pepco Schedule R tariff,[4] which varies between $0.098 per kWh in winter and $0.104 per kWh in summer.

Prior to solving the day-ahead market, HEMS submit their bids for all settlement periods (i.e., 96 periods at a 15-minute settlement interval). A HEMS can submit a mix of supply and demand bids, so long as supply and demand bids are not submitted for the same settlement period. Moreover, within a settlement period, multiple demand bids (i.e., fixed and variable demand) or supply bids (i.e., PV and battery) can be submitted. Fixed demand bids must be bid at the ceiling price, otherwise bids can be priced anywhere between the floor and ceiling price. The day-ahead market constructs supply and demand curves from these bids and independently resolves settlement prices for all settlement periods. The outcome of one settlement period does not influence the outcome of any other period.

In constructing the demand curve, the uncontrollable load quantity is first put into the stack at the ceiling price. Subsequently, all fixed demand bids are also added at the ceiling price. Finally, variable load bids are added to the demand curve in order of descending price. To construct the supply curve, supply bids are first added in ascending order by price. If the total supply quantity is less than the total demand, then a utility bid at the ceiling price is added at a sufficient quantity to recuperate this difference.

The day-ahead market finds the day-ahead settlement price through the intersection of the supply and demand curves for all settlement prices. Demand bids with a price at or above the settle price, and supply bids at or below the settle price are approved by the market. Then, the settle

---

[4] https://www.pepco.com/MyAccount/MyBillUsage/Documents/Updated%20060120%20-%20R.pdf

price is established, the bids are either approved or rejected by the market and are communicated back to the HEMS federates via HELICS.

3.2.2 Real-Time Market Solver

Every hour on the hour (in simulation time), the real-time solver solves the market at 15-minute settlement periods. The real-time market solves for all hours included in the HEMS forecast (i.e., current and future), but only the resolution of the current hour is binding. For example, at 12 a.m., each HEMS will submit real-time bids for all hours through 8 a.m. All settlement prices, including possible surplus pricing interventions, will be communicated back to the HEMS, but only the bids for the 12 a.m. hour will be considered finalized.

The real-time solver constructs supply and demand curves in much the same way as for the day-ahead market. However, the ceiling price for the real-time market is tied to the settled day-ahead price instead of the cost recovery-based retail rate.

The real-time market may override settled prices with surplus pricing when the possibility of feeder export is elevated. In this preliminary implementation, surplus pricing is activated when there is some quantity of supply bid into the market, and the ratio of total demand (i.e., fixed and variable) to total supply quantity (i.e., PV and battery) is less than 1.3. Surplus pricing applies a surplus factor to the settled day-ahead prices as shown below in Equation (1) that decreases the price (and may even drive it negative).

$$\text{Surplus Factor} = (\Sigma Q_{\text{demand, kWh}} / \Sigma Q_{\text{supply, kWh}}) - 1 \qquad (1)$$

Surplus pricing in a forecast is intended to simultaneously signal to the HEMS that (a) exporting to the grid is discouraged, and (b) increasing flexible demand is encouraged. Results from this study will demonstrate if the signal is effective in steering HEMS optimization such that forecasted surplus pricing in future non-binding periods dissipates when the period finally comes to pass.

3.2.3 Day-Ahead and Real-Time Market Settlement

The day-ahead market is binding, approved demand and supply bids can calculate costs (or revenue) from Equation (2). Note that negative results indicate a cost and positive results indicate revenue to the customer in this equation.

$$\$ = (Q_{\text{supply, kWh}} - Q_{\text{demand, kWh}}) \times P_{\text{settle, \$/kWh}} \qquad (2)$$

Because each 15-minute day-ahead settlement period in this implementation perfectly overlaps with a real-time settlement period, real-time market imbalances (i.e., the additional amount a customer must pay or be paid) can be resolved according to Equation (3), shown below.

$$\$ = [(Q_{\text{RT supply, kWh}} - Q_{\text{DA supply, kWh}}) - (Q_{\text{RT demand, kWh}} - Q_{\text{DA demand, kWh}})] \times P_{\text{RT, \$/kWh}} \qquad (3)$$

Recall that the day-ahead market is binding such that costs from demand bids and revenue from supply bids have been paid by the time the real-time market solves. Equation (3) accounts for possible deviations from the approved day-ahead market bid. To help clarify this point, consider a case where the same supply bid price and quantity pair is bid into and approved in the day-ahead and real-time markets for the same 15-minute period. This seller will be paid at the day-ahead settlement price and receive no compensation at the real-time settlement price. However, in the scenario where the approved real-time supply bid quantity had been twice that of the approved day-ahead supply bid, then the seller would only get paid for half his or her real-time quantity at the settled real-time price (the other half would be paid at the day-ahead settle price).

4 Home Energy Management System

4.1 foresee

foresee^{TM} is a user-centric home energy management system that is capable of managing the behind-the-meter DERs—including PV, batteries, controllable loads—and provide grid services based on utility or market signals (Jin et al. 2017). **foresee** is formulated as a multi-objective model predictive control framework. The objectives include minimization of utility cost, user discomfort, and battery degradation. The multi-objective optimization framework allows us to consider the differences in the various user preferences of the occupants. For example, some occupants may prefer to reduce cost while tolerating minor discomfort in terms of room temperature, whereas some occupants may be willing to pay more to ensure maximum comfort. A Simple Multi-Attribute Rating Technique Exploiting Ranks (SMARTER) method is used in **foresee** to elicit user preferences, which can be done during the initial deployment of **foresee**.

4.2 Market Participation

foresee calculates the bids, with each bid consisting of a price ($) and quantity (kWh) pair, to participate in the day-ahead and real-time market. The bids submitted to the market can be broadly classified into demand bids and supply bids. It is noteworthy that **foresee** submits either a demand or supply bid for each timestep. Demand bids can be further classified as firm demand bids and flexible demand bids. Firm demand bids signify the desired load of the house, including uncontrollable loads and HVAC and water heating loads to maintain user comfort. Similarly, flexible demand bids represent the additional flexibility offered by the DERs in the house. Supply bids can also be further classified as PV supply bids and battery supply bids, depending on which DER is bidding to export to the grid.

To calculate bids for market participation, **foresee** first quantifies the demand flexibility of the houses. **foresee** solves a multi-objective optimization problem to compute the flexibility band (Munankarmi et al. 2020), shown in Figure 5, considering the user preferences and physical constraints. The nominal trajectory of the flexibility band, which is same as HEMS-only operation, represents the desired HEMS trajectory considering the utility tariff and user inconvenience. The upper and lower trajectory represents the maximum and minimum desired load profile considering the flexibility of all behind-the-meter resources.

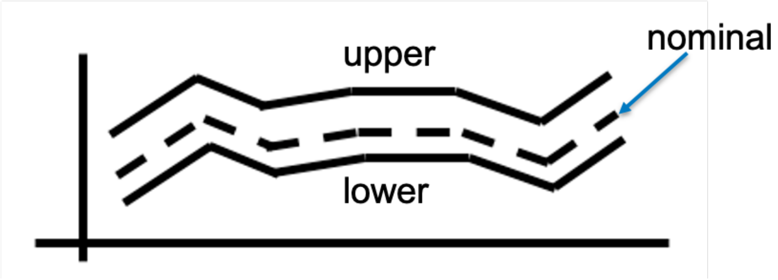

Figure 5. Overview of flexibility band.

For determining whether to bid a demand or supply bid at any timestep, the nominal trajectory of the flexibility band is used. **foresee** determines the demand mode and submits demand bids when the net power of house is positive ($P_t^g \geq 0$) signifying net demand in the house. An example flexibility band is shown in Figure 6. The firm demand quantity at any timestep is provided by the nominal trajectory of the flexibility band. It includes the uncontrollable load and optimal scheduling of behind-the-meter resources per price signals considering user convenience. On the other hand, flexible demand quantity is considered as the difference between upper and nominal trajectory.

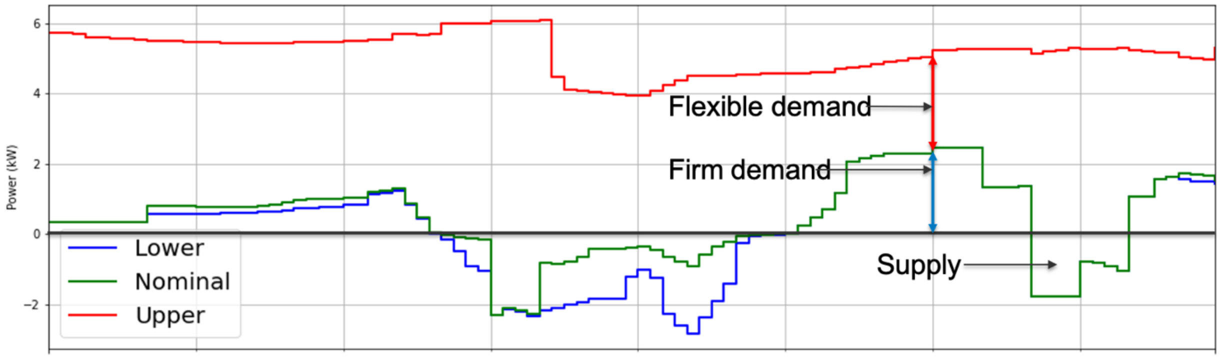

Figure 6. An example of flexibility band.

Similarly, **foresee** determines supply mode and submits supply bids when the net power of the house is negative ($P_t^g < 0$), signifying net export from the house. The nominal trajectory is used for bidding the PV and battery supply bid quantities. For PV, the power flow of PV to grid, load, and battery is tracked in optimization and PV power to grid is bid as PV bid quantity in the market. Similarly, battery charge power as well as battery discharge power to grid and load is tracked in optimization. Battery discharge power to the grid is submitted as battery supply quantity in the market.

4.2.1 Day-Ahead Market Bidding

For formulating the day-ahead bids, **foresee** solves a multi-objective model predictive control problem where the objectives include minimization of utility cost, user discomfort, battery degradation, and maximization of flexibility band. **foresee** receives the wholesale and retail price for computing the utility cost in the optimization formulation. Mathematically, the objective function of day-ahead market **foresee** formulation can be represented as follows:

$$
\begin{aligned}
min \sum_{t} \{ \lambda_t^{wholesale} b^{m} & \left(P_{t,grid,o}^{pv} + P_{t,grid,o}^{batt}\right) \\
& + \lambda_t^{\mathrm{retail}} \mathrm{b}^{\mathrm{m}} \left(\mathrm{P}_{\mathrm{t,o}}^{\mathrm{hvac}} + \mathrm{P}_{\mathrm{t,o}}^{\mathrm{wh}} + \mathrm{P}_{\mathrm{t,o,load}}^{\mathrm{batt}} + \mathrm{P}_{\mathrm{t,o,chg}}^{\mathrm{batt}} + \mathrm{P}_{\mathrm{t,o}}^{\mathrm{unctrl}} + \mathrm{P}_{\mathrm{t,load,o}}^{\mathrm{pv}} \right. \\
& \left. + \mathrm{P}_{\mathrm{t,batt,o}}^{\mathrm{pv}}\right) + b^{fb}\left[\left(P_{t,V}^{g} - P_{t,o}^{g}\right) + \left(Q_{t,V}^{g} - Q_{t,o}^{g}\right)\right] \\
& + b^{fb}\left[\left(P_{t,o}^{g} - P_{t,\Lambda}^{g}\right) + \left(Q_{t,o}^{g} - Q_{t,\Lambda}^{g}\right)\right] \\
& + b^{air}\left[\left(T_{t,o}^{air} - \overline{T}_{o}^{air}\right)^{2} + \left(\underline{T}_{o}^{air} - T_{t,o}^{air}\right)^{2}\right] \\
& + b^{wt}\left[\left(T_{t,o}^{wh} - \overline{T}_{o}^{wh}\right)^{2} + \left(\underline{T}_{o}^{wh} - T_{t,o}^{wh}\right)^{2}\right] + b^{batt}\left(P_{t,o}^{ch} - P_{t,o}^{dis}\right) \\
& + b^{air}\left[\left(T_{t,\Lambda}^{air} - \overline{T}_{\Lambda}^{air}\right)^{2} + \left(\underline{T}_{\Lambda}^{air} - T_{t,\Lambda}^{air}\right)^{2}\right] \\
& + b^{wt}\left[\left(T_{t,\Lambda}^{wh} - \overline{T}_{\Lambda}^{wh}\right)^{2} + \left(\underline{T}_{\Lambda}^{wh} - T_{t,\Lambda}^{wh}\right)^{2}\right] + b^{batt}\left(P_{t,\Lambda}^{ch} - P_{t,\Lambda}^{dis}\right) \\
& + b^{air}\left[\left(T_{t,V}^{air} - \overline{T}_{V}^{air}\right)^{2} + \left(\underline{T}_{V}^{air} - T_{t,V}^{air}\right)^{2}\right] \\
& + b^{wt}\left[\left(T_{t,V}^{wh} - \overline{T}_{V}^{wh}\right)^{2} + \left(\underline{T}_{V}^{wh} - T_{t,V}^{wh}\right)^{2}\right] + b^{batt}\left(P_{t,V}^{ch} - P_{t,V}^{dis}\right)
\end{aligned}
\tag{4}
$$

where, the subscript o represents the nominal trajectory, V represents the lower trajectory, and Λ represents the upper trajectory of the flexibility band. P_t^g and Q_t^g represent the net active and reactive power of the house. $b^m, b^{fb}, b^{air}, b^{wt}, and\ b^{batt}$ represent the weighting factor for different objectives—i.e., minimizing utility cost, maximizing flexibility band, minimizing air and water discomfort, and minimizing battery degradation, respectively.

The first and second term of the objective function represents the utility cost. $\lambda_t^{wholesale}$ is the wholesale market price; λ_t^{retail} is the retail market price; $P_{t,grid,o}^{pv}$ is PV power to grid; $P_{t,grid,o}^{batt}$ is battery discharge power to the grid; $P_{t,o}^{hvac}$ is HVAC power; $P_{t,o}^{wh}$ is WH demand; $P_{t,o,load}^{batt}$ is battery discharge power to the load; $P_{t,o,chg}^{batt}$ is battery charge power; $P_{t,o}^{unctrl}$ is uncontrollable load; $P_{t,load,o}^{pv}$ is PV power to load; $P_{t,batt,o}^{pv}$ is PV power to battery. The PV and battery discharge to the grid is compensated at wholesale price whereas the load demand from the grid as well as PV and battery power to house load is compensated at retail price. This encourages the building to self-consume the excess power it generates before exporting to the grid.

The third and fourth term represents the maximization of flexibility band. The fifth term represents the penalty for indoor air temperature discomfort. T_t^{air} is indoor air temperature whereas $\overline{T}^{air}$ and $\underline{T}^{air}$ represent maximum and minimum desired indoor air temperature. Similarly, the sixth and seventh term represent penalties for water temperature discomfort and battery usage. Here, T_t^{wh} represents water temperature inside the tank; $\overline{T}^{wh}$ and $\underline{T}^{wh}$ represent the maximum and minimum desired water temperature; and P_t^{ch} and P_t^{dis} represent total battery charging and discharging power. The penalty increases quadratically as indoor air temperature and hot water temperature deviate from the comfort band.

The optimization problem is subject to individual device constraints and whole home power constraints. Readers can refer to (Munankarmi et al. 2020) for details on HVAC and WH constraints.

PV constraints are represented as follows:

$$\overline{P}_t^{pv} \leq P_t^{pv} \leq 0 \tag{5a}$$

$$\left(P_t^{pv}\right)^2 + \left(Q_t^{pv}\right)^2 \leq \left(\overline{S}^{pv}\right)^2 \tag{5b}$$

$$-\overline{\gamma}^{pv} P_t^{pv} \leq Q_t^{pv} \leq \overline{\gamma}^{pv} P_t^{pv} \tag{5c}$$

$$-P_t^{load} \leq P_{t,load}^{pv} \leq 0 \tag{5d}$$

$$-P_t^{ch} \leq P_{t,batt}^{pv} \leq 0 \tag{5e}$$

$$P_{t,grid}^{pv} \leq 0 \tag{5f}$$

$$P_t^{pv} = P_{t,load}^{pv} + P_{t,batt}^{pv} + P_{t,grid}^{pv} \tag{5g}$$

Equation (5a) ensures that the PV power production (P_t^{pv}) is between 0 and the maximum PV power available $(\overline{P}_t^{pv})$. Similarly, equation (5b) ensures that the total PV apparent power is within the inverter capacity $(\overline{S}^{pv})$. In equation (5c), the reactive power of PV (Q_t^{pv}) is constrained between fraction of PV active power (P_t^{pv}) guided by positive constant $(\overline{\gamma}^{pv})$. $(\overline{\gamma}^{pv})$ is computed based on the power factor limit of the PV inverter. Equation (5d) guarantees that the PV power to load $(P_{t,load}^{pv})$ does not exceed the total load of the house (P_t^{load}). Similarly, Equation (5e) guarantees that the PV power to battery $(P_{t,batt}^{pv})$ does not exceed the battery charging requirement (P_t^{ch}). Equation (5g) ensures that the total PV power is the sum of PV power to grid, battery, and load.

Battery constraints are represented in equations (6a) through (6g):

$$B_t = B_{t-1} + \Delta t \left(\eta^{ch} P_t^{ch} + \frac{P_t^{dis}}{\eta^{dis}} \right) \tag{6a}$$

$$\underline{B} \leq B_t \leq \overline{B} \tag{6b}$$

$$0 \leq P_t^{ch} \leq \overline{P}^{ch} \tag{6c}$$

$$\overline{P}^{dis} \leq P_t^{dis} \leq 0 \tag{6d}$$

$$\overline{P}^{dis} \leq P_{grid,t}^{dis} \leq 0 \tag*{(6d)}$$

$$\overline{P}^{dis} \leq P_{load,t}^{dis} \leq 0 \tag{6e}$$

$$P_{grid,t}^{dis} \geq -P_t^{load} \tag{6f}$$

$$P_{grid,t}^{dis} + P_{load,t}^{dis} = P_t^{dis} \tag{6g}$$

Equation (6a) represents the simplified battery model used for model predictive control of the battery. In this model, battery state of charge (SOC), B_t, depends on initial battery SOC (B_{t-1}), charging power (P_t^{ch}), and battery discharging power (P_t^{dis}). η^{ch} and η^{dis} represent battery charging and discharging efficiency, and Δt represents simulation timestep. Equation (6b) guarantees that the battery SOC is within minimum ($\underline{B}$) and maximum ($\overline{B}$) permissible SOC. Equation (6c) ensures that the battery charging power (P_t^{ch}) is within maximum charging power limit ($\overline{P}^{ch}$). Equations (6d), (6e), and (6f) ensure that the total battery discharge (P_t^{dis}), discharge to grid ($P_{grid,t}^{dis}$), and discharge to load ($P_{load,t}^{dis}$) are within maximum discharging ($\overline{P}^{dis}$) power limits. Equation (6g) guarantees that the battery discharge to load does not exceed the total load of the house (P_t^{load}).

Total house power constraints are represented with the following equations:

$$P_t^g = P_t^{pv} + \left(I_t^c \overline{P}^c + I_t^h \overline{P}^h\right) + I_t^T P_t^{wh} + \left(P_t^{ch} + P_t^{dis}\right) + P_t^{unctrl} \tag{7a}$$

$$P_t^{load} = P_t^{hvac} + P_t^{wh} + P_t^{unctrl} \tag{7b}$$

$$P_{t,load}^{pv} + P_{t,load}^{dis} \geq -P_t^{load} \tag{7c}$$

$$P_{t,grid}^{pv} + P_{t,grid}^{dis} \leq P_t^g \tag{7d}$$

Equation (7a) computes the net house power (P_t^g) as sum of all demand and generation in the house. Similarly, Equation (7b) represents that the total load of house (not accounting battery charge power) is sum of load of the house (HVAC, WH, and uncontrollable load). Equation (7c) guarantees that the total power from PV and battery to the load does not exceed the total load of the house (P_t^{load}). Equation (7d) ensures that the during export, the total power export to the grid is sum of battery discharge and PV power to the grid.

Flexibility band constraints are represented as follows:

$$P_{t,V}^g \leq P_{t,o}^g \leq P_{t,\Lambda}^g \tag{8}$$

Equation (8) ensures the nominal power $P_{t,o}^g$ lies within the flexibility band ($P_{t,V}^g, P_{t,\Lambda}^g$).

For the day-ahead bids, the firm bid is submitted with retail price and flexible bid is submitted with wholesale price. PV supply bids are submitted with wholesale price. Battery supply bids are submitted with retail price.

4.2.2 Real-Time Market Bidding

The objective of the real time formulation includes minimization of deviation from the day-ahead schedule, user inconvenience, battery degradation, and maximization of the flexibility band. In real-time formulation, the day-ahead cleared price is used to calculate the utility cost. Mathematically, the objective of real-time formulation can be defined as:

$$
\begin{aligned}
min\sum_{t}\{ \lambda_t^{da} b^m & \left(\left(P_{t,grid,o}^{pv,rt} - P_{t,grid,o}^{pv,da}\right) * 0.8 + \left(P_{t,load,o}^{pv,rt} - P_{t,load,o}^{pv,da}\right) + \left(P_{t,batt,o}^{pv,rt} - P_{t,batt,o}^{pv,da}\right)\right) \\
& + \lambda_t^{da} b^m \left(\left(P_{t,grid,o}^{dis,rt} - P_{t,grid,o}^{dis,da}\right) * 0.8 + \left(P_{t,dis,o}^{pv,rt} - P_{t,dis,o}^{pv,da}\right) + \left(P_{t,o}^{ch,rt} - P_{t,o}^{ch,da}\right)\right) \\
& + \lambda_t^{da} b^m \left(P_{t,load,o}^{rt} - P_{t,load,o}^{da}\right) + b^{fb}\left[\left(P_{t,V}^{g} - P_{t,o}^{g}\right) + \left(Q_{t,V}^{g} - Q_{t,o}^{g}\right)\right] \\
& + b^{fb}\left[\left(P_{t,o}^{g} - P_{t,\Lambda}^{g}\right) + \left(Q_{t,o}^{g} - Q_{t,\Lambda}^{g}\right)\right] + b^{air}\left[\left(T_{t,o}^{air} - \overline{T}_{o}^{air}\right)^2 + \left(\underline{T}_{o}^{air} - T_{t,o}^{air}\right)^2\right] \\
& + b^{wt}\left[\left(T_{t,o}^{wh} - \overline{T}_{o}^{wh}\right)^2 + \left(\underline{T}_{o}^{wh} - T_{t,o}^{wh}\right)^2\right] + b^{batt}\left(P_{t,o}^{ch} - P_{t,o}^{dis}\right) \\
& + b^{air}\left[\left(T_{t,\Lambda}^{air} - \overline{T}_{\Lambda}^{air}\right)^2 + \left(\underline{T}_{\Lambda}^{air} - T_{t,\Lambda}^{air}\right)^2\right] \\
& + b^{wt}\left[\left(T_{t,\Lambda}^{wh} - \overline{T}_{\Lambda}^{wh}\right)^2 + \left(\underline{T}_{\Lambda}^{wh} - T_{t,\Lambda}^{wh}\right)^2\right] + b^{batt}\left(P_{t,\Lambda}^{ch} - P_{t,\Lambda}^{dis}\right) \\
& + b^{air}\left[\left(T_{t,V}^{air} - \overline{T}_{V}^{air}\right)^2 + \left(\underline{T}_{V}^{air} - T_{t,V}^{air}\right)^2\right] \\
& + b^{wt}\left[\left(T_{t,V}^{wh} - \overline{T}_{V}^{wh}\right)^2 + \left(\underline{T}_{V}^{wh} - T_{t,V}^{wh}\right)^2\right] + b^{batt}\left(P_{t,V}^{ch} - P_{t,V}^{dis}\right) \qquad (9)
\end{aligned}
$$

Here, superscript rt denotes the real-time optimization variable whereas da denotes the day-ahead parameters. λ_t^{da} represents the day-ahead cleared price received from market. As excess demand and export compared to day-ahead scheduling is billed in real-time, the utility cost represented by the first to third term of the objective function accounts for utility cost in real-time. A factor of 0.8 is used for the deviation of export of PV and battery power to grid to prioritize self-consumption of PV and battery energy within the house. In the real-time formulation, we need to consider whether the bids submitted in real-time are accepted or not. We account for this prior to real-time optimization by setting any unsettled PV and battery da quantity as 0 if not accepted.

4.2.3 Real-Time Market Dispatch

When implementing the real-time bids and dispatching associated control actions for each DER, we need to consider whether a particular bid was accepted in the market or not. For the firm and supply bids, **foresee** implements the control actions associated with nominal trajectory when the firm bids are approved in the market. It is worth mentioning that the firm quantity, which includes the uncontrollable loads, needs to be approved in the market and thus is always priced at the ceiling price. In case of the flexible bid demand, **foresee** implements the control variable associated with the upper trajectory of the flexible band if the flexible demand bid is approved. When the flexible demand bids are not approved, then no action is taken. In cases where both firm and flexible bids are accepted in the market, it implements the flexible demand bids because a flexible demand bid represented by upper trajectory also includes the firm quantity.

For the PV supply bids, the control actions of each DER associated with the nominal trajectory are implemented with $P_{t,grid}^{PV} = P_{t,grid}^{PV}$ if the PV supply bids are approved and $P_{t,grid}^{PV} = 0$ if the PV supply bids are not approved. Similarly, for the battery supply bids, the control variables of each DER associated with nominal trajectory are implemented with $P_{t,grid}^{batt} = P_{t,grid}^{batt}$ if the battery supply bids are approved and $P_{t,grid}^{batt} = 0$ if the battery supply bids are not approved.

5 Blockchain

5.1 EW-DOS Components

The co-simulation application integrates the Energy Web Decentralized Operating System (EW-DOS) stack developed by EWF, a non-profit organization maintaining open-source blockchain tools for the energy domain. EWF's digital ledger, the Energy Web Chain (EWC), is one of the core components of EW-DOS and has been leveraged for record keeping in this project. The EW-DOS provides the foundation upon which various applications and services can run to connect participants in the energy sector. EW-DOS currently facilitates renewable energy and carbon markets and the management of DERs on the grid.

Decentralized Identifiers (DIDs) are unique identifiers for each entity created and stored in the identity directory of EW-DOS. The DIDs are public-private key pairs, and can also be used to store more information about the specific characteristics of the entity, and can be verified by other parties. The market and the participants use the DIDs to authenticate entities engaging in an energy application or service (i.e., a distributed energy system owner providing services to the grid). DIDs can be interconnected by an entity delegating authority to other DIDs (i.e., a solar panel delegating control authority to its owner). A key advantage of DIDs is that they are interoperable across multiple systems (i.e., utility and distribution system management applications).

5.2 Integration

In this simulation, a DID is created for the market, each homeowner, HEMS, and all DERs. The DERs and the homeowner are added as delegates to the DID for each respective building's HEMS. Figure 7 shows the proof of DID created for a DER and assigned as a delegate to the HEMS, so the HEMS can make claims or bids on behalf of the DER. Note, establishing a DID requires funds, so a "master" DID account is also established to faucet funds to newly created DIDs for simulation purposes.

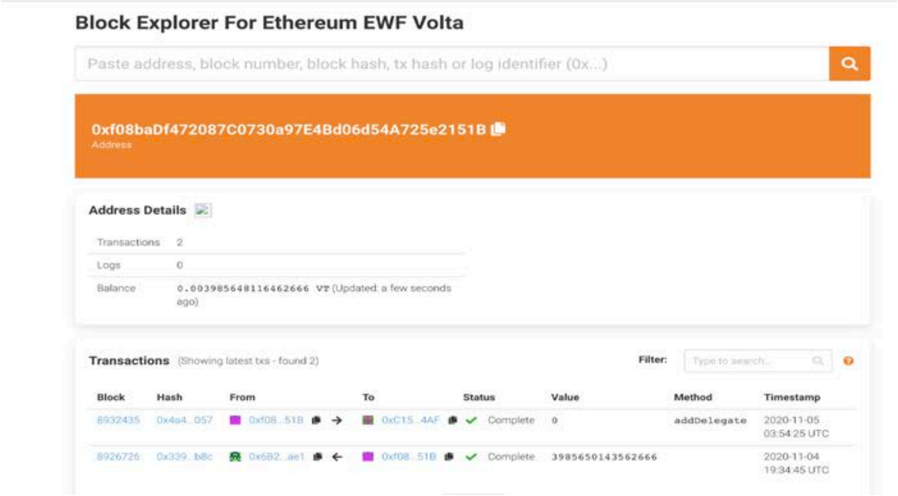

Block Explorer For Ethereum EWF Volta

0xf08baDf472087C0730a97E4Bd06d54A725e2151B
Address

Address Details

Transactions	2
Logs	0
Balance	0.003985648116462666 VT (Updated: a few seconds ago)

Transactions (Showing latest txs - found 2)

Block	Hash	From		To	Status	Value	Method	Timestamp
8932435	0x4a4...057	0xf08...51B	→	0xC15...4AF	✓ Complete	0	addDelegate	2020-11-05 03:54:25 UTC
8926726	0x339...b8c	0x6B2...ae1	←	0xf08...51B	✓ Complete	3985650143562666		2020-11-04 19:34:45 UTC

Figure 7. Screenshot showing the DID creation of a DER delegated to its homeowner.

Within the simulation, DIDs are used to authenticate data that HEMS sends to the market and vice versa. Importantly, as the simulation is instantiated, the addresses of the market and all HEMS are made known to each other. This is easily accomplished through preprocessing in simulation; in the real world, a digital directory could provide similar functionality. With knowledge of a sender's address, a sender's public key can be programmatically pulled from the identity directory and in turn used to verify an encrypted signature that the sender passed along to a recipient. If the signature matches the sender's data and public key, a recipient knows the data has come from the sender.

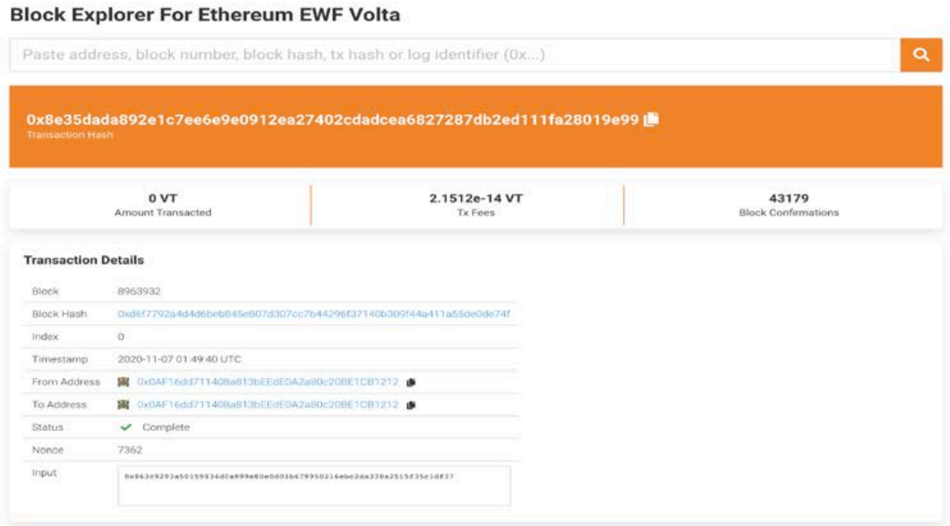

Block Explorer For Ethereum EWF Volta

0x8e35dada892e1c7ee6e9e0912ea27402cdadcea6827287db2ed111fa28019e99
Transaction Hash

0 VT	2.1512e-14 VT	43179
Amount Transacted	Tx Fees	Block Confirmations

Transaction Details

Block	8963932
Block Hash	0xd6f7792a4d4d6beb845e807d307cc7b44296f37140b309f44a411a55de0de74f
Index	0
Timestamp	2020-11-07 01:49:40 UTC
From Address	0x0AF16dd711408a813bEEdE0A2a80c20BE1CB1212
To Address	0x0AF16dd711408a813bEEdE0A2a80c20BE1CB1212
Status	✓ Complete
Nonce	7362
Input	

Figure 8. Screenshot of approved bids data hash embed on the EWC.

In this simulation the market periodically posts a transaction to the EWC with the hash of the approved bids (hashed using the SHA-256 cryptographic hash algorithm) for record as shown in Figure 8. Note, this transaction requires marginal funds so the account must be seeded with sufficient funds.

6 Experimentation

6.1 Experimental Setup

A co-simulation application built using the HELICS (Palmintier et al. 2019) framework is used to perform the experiments on the feeder. This agent-based platform facilitates a coordinated simulation of the individual simulation tools described above in simulation time and also provides communication between modules using the ZeroMQ protocol.

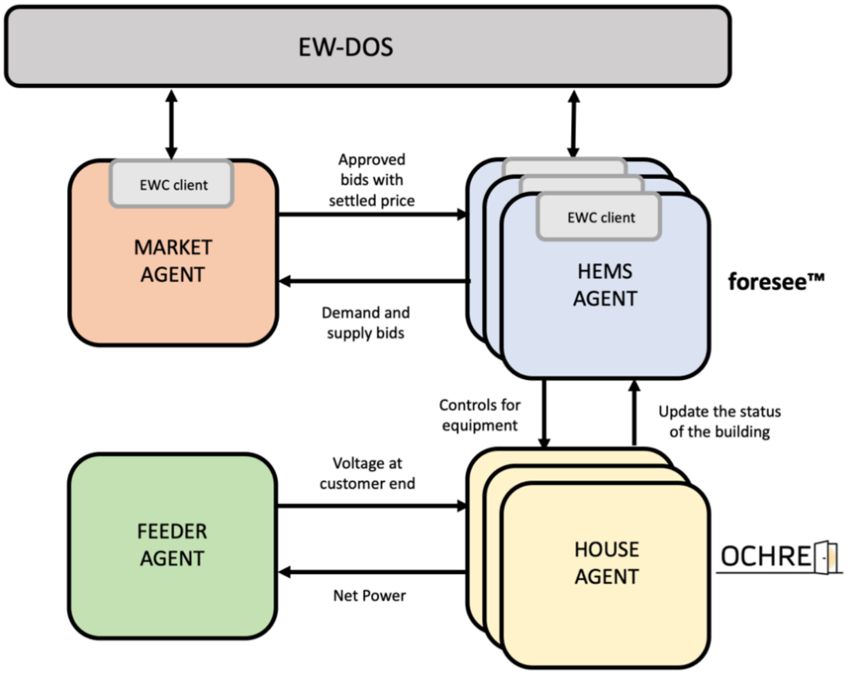

Figure 9. Co-simulation architecture.

Figure 9 illustrates the architecture of the co-simulation. Its highly modular structure allows for easy simulation of the experimental scenarios with different combinations of agents. There is a separate agent for market and feeder modules and an individual house and HEMS agent for the individual market participants. Agent types include:

- Feeder Agent: Runs the feeder model at a one-minute timestep using OpenDSS and a Python interface. At each timestep, the agent will receive the power consumed by each building on the feeder and update the state of the feeder.
- House Agent: Simulates the house model at a one-minute timestep using OCHRE, based on the controls received from the HEMS agent. At each timestep, it updates the HEMS system on the status of appliances and the feeder agent of the consumed power.
- HEMS Agent: Runs the **foresee** optimizer for an individual building based on the status received from the house model and approved bids from the market at a 15-minute timestep. The optimized controls are sent to the house agent for implementation.

- Market Agent: Solves the market based on the bids placed by HEMS at a 15-minute timestep. The settled prices and the approved bids are communicated to the HEMS along with DIDs. Using the EWC client, it posts the hashed values of market decisions on the chain.

6.2 Scenarios

The six scenarios in Table 1 were simulated to study the performance of the feeder under different market structures and different levels of DER (PV and battery) penetration. The simulations are performed for six consecutive days in the shoulder season since it is a challenging season with moderate PV and low cooling load.

Table 1. List of Experimental Scenarios

Scenario	Include HEMS	Market Type	DER penetration
1a	No	Time-of-use (TOU)	Business as usual (BAU)
1b	No	TOU	100% DER penetration (100P)
2a	Yes	TOU	BAU
2b	Yes	TOU	100P
3a	Yes	Market	BAU
3b	Yes	Market	100P

Scenarios 1a and 1b are baseline runs to obtain the data for the BAU case and 100% DER penetration, simulating only the feeder and the house models without any external controls. These scenarios are helpful in understanding the performance of the feeder under increased DER penetration without any coordination.

Scenarios 2a and 2b have the HEMS deployed in each of the residential buildings with different DER penetrations. Under both scenarios, HEMS will be operating under the pilot TOU pricing optimizing for the individual houses without any coordination among the buildings.

Scenarios 3a and 3b are market scenarios, where the HEMS will be participating in the market and optimizing for the house based on the market settlement. The BAU case and the 100% DER penetration case showcase the ability of the market to enable net zero export on the primary feeder head by coordinating the DER.

6.3 DER Sizing

6.3.1 PV Sizing

The actual PV size of the buildings in the feeder is adopted for the BAU cases (scenarios 1a, 2a, and 3a). The total PV capacity of the feeder for BAU cases is 257 kW. For the 100P cases, we employed a top-down approach for determining the PV capacity of the feeder and each house. The PV sizing for each house is performed using the following steps:

a. Determination of feeder PV capacity: First, the total PV capacity of the feeder is determined for 100P cases. We considered the total PV capacity of the feeder as the minimum daytime load of the annual peak day of the feeder. The minimum daytime load of the feeder on a peak load day was 4.25 MW. Thus, the total PV capacity in the feeder for 100P cases was 4.25 MW.

b. Determination of house PV size: The PV capacity of each house is scaled based on the annual energy consumption of the house. This results in houses with higher consumption having higher PV capacity. For the homes equipped with PV in BAU cases, the PV size for the 100P case is kept as in BAU cases.

c. The maximum PV size limit for each residential house is set to 12 kW and the size of PV in each house is in increments of 0.3 kW, which is the typical size of the PV module. As a result, few homes assigned with PV size greater than 12 kW (from step (b)) were limited to 12 kW of PV. Thus, the total feeder PV capacity for 100P was 4.05 MW.

The distribution of the PV sizes in the BAU and 100P cases is presented in Figure 10.

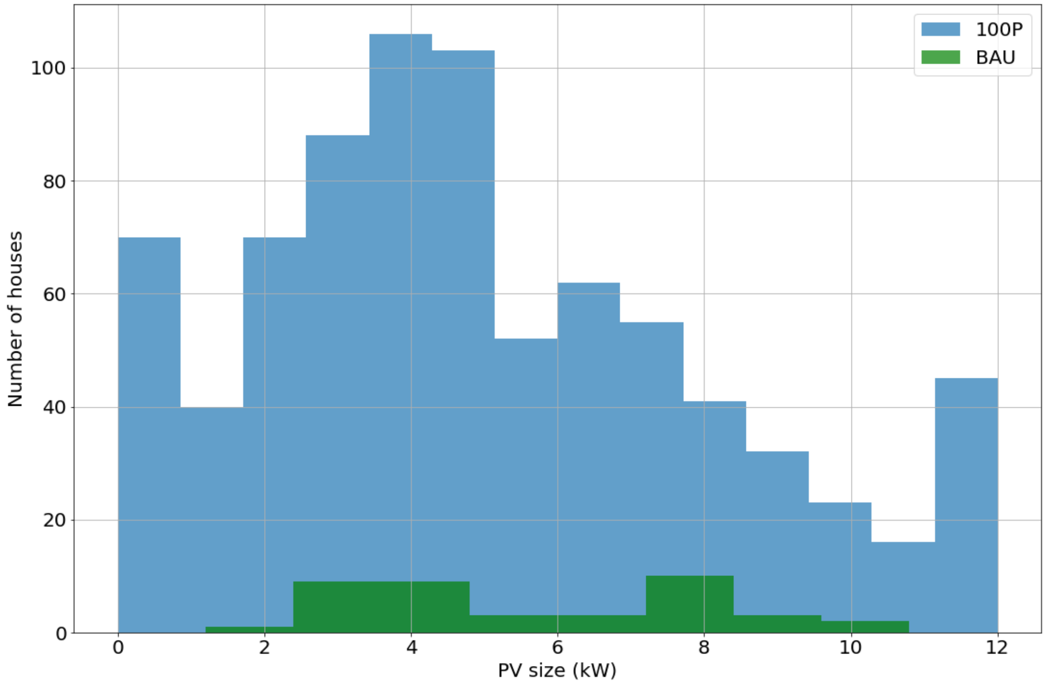

Figure 10. Distribution of PV size.

6.3.2 Battery Sizing

For the BAU cases, the total battery size is 0 kWh as batteries were not available in the buildings on the feeder. For 100P cases, we considered a commercially available battery, Tesla Powerwall, and used the specification of the Powerwall. The battery size is assigned depending on the PV size of the homes. The homes with PV capacity greater than 6 kW were equipped with Tesla

Powerwall 2 (13.5 kWh capacity) whereas the homes with PV capacity less than 6 kW were equipped with Tesla Powerwall 1 (6.4 kWh). The total battery capacity of the feeder was 6.76 MWh.

7 Result Analysis

The results from the six scenarios are analyzed to show the performance of the feeder and the house models under different operating conditions and the significant improvement gained by adding the market into the system.

7.1 Feeder Analysis

The feeder analysis shows the net power and voltage results from the scenarios. At the end of the section, we report all power and voltage metrics for each scenario, including net feeder energy, maximum import and export, and voltage violations.

The net power at the feeder head for selected shoulder season baseline scenarios is shown in Figure 11. Net power includes all modeled residential loads, BAU PV, and unmodeled commercial loads and PV. The BAU scenario peak power exceeds 1.5 MW on multiple days, and the minimum power was about 200 kW, indicating that there was no grid export at the feeder head. The 100% DER penetration scenario included significantly more PV, and there was grid export for some of the days. The maximum grid export was about 2.1 MW.

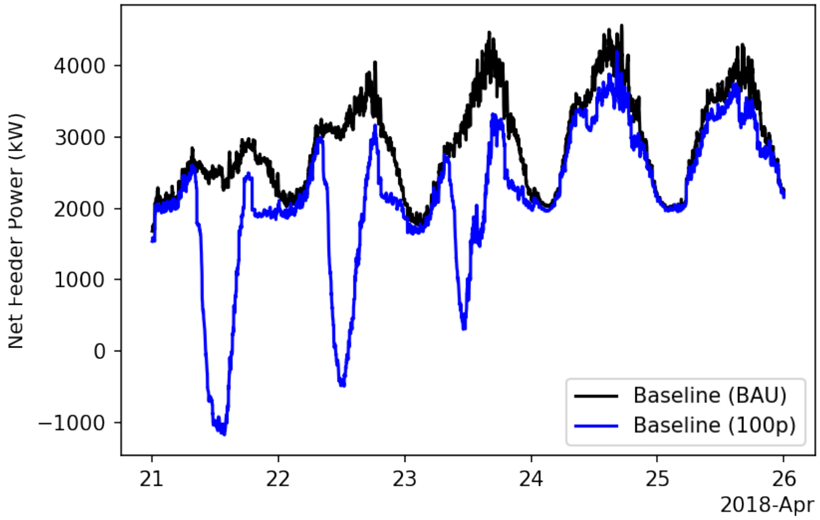

Figure 11. Net power at the feeder head for the baseline business-as-usual and 100% DER penetration scenarios.

Voltages for the shoulder season baseline 100% penetration scenario are shown in Figure 12. Most voltages stay within the American National Standards Institute (ANSI) voltage limits of 0.95 to 1.05 per unit (p.u.) However, some voltages exceed 1.05 p.u. during days with high PV penetration.

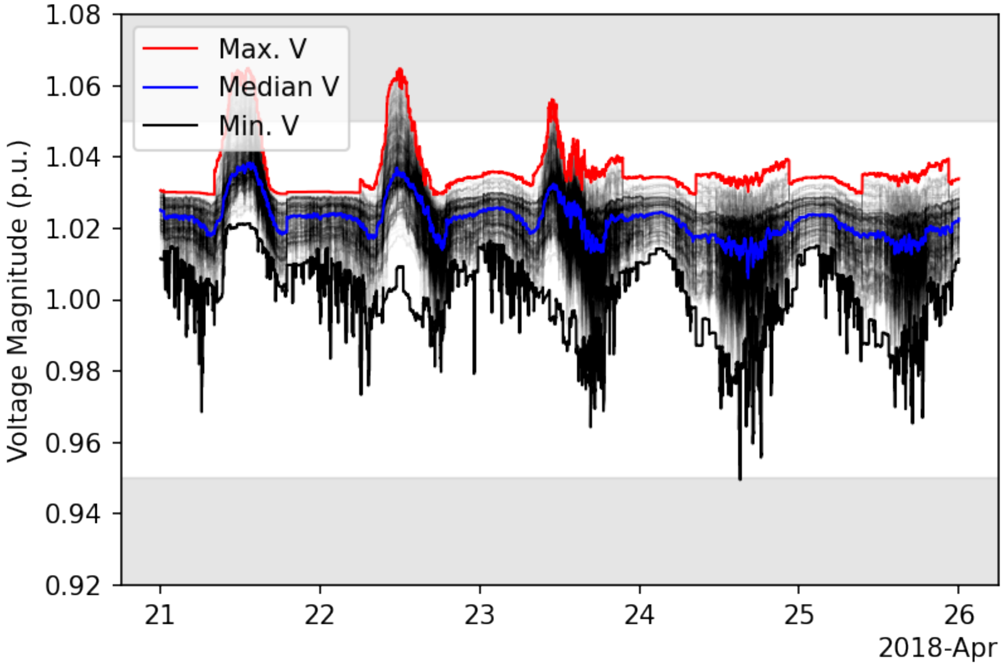

Figure 12. Community voltages for the baseline 100% DER penetration scenario.

Incorporating HEMS significantly changes the load profile at the feeder head. Figure 13 shows the net power at the feeder head for the baseline and HEMS scenarios with 100% DER penetration in the shoulder season. The HEMS scenarios are designed to follow the TOU rate, which leads to more grid export during the peak TOU period and more grid import at off-peak times, especially at night.

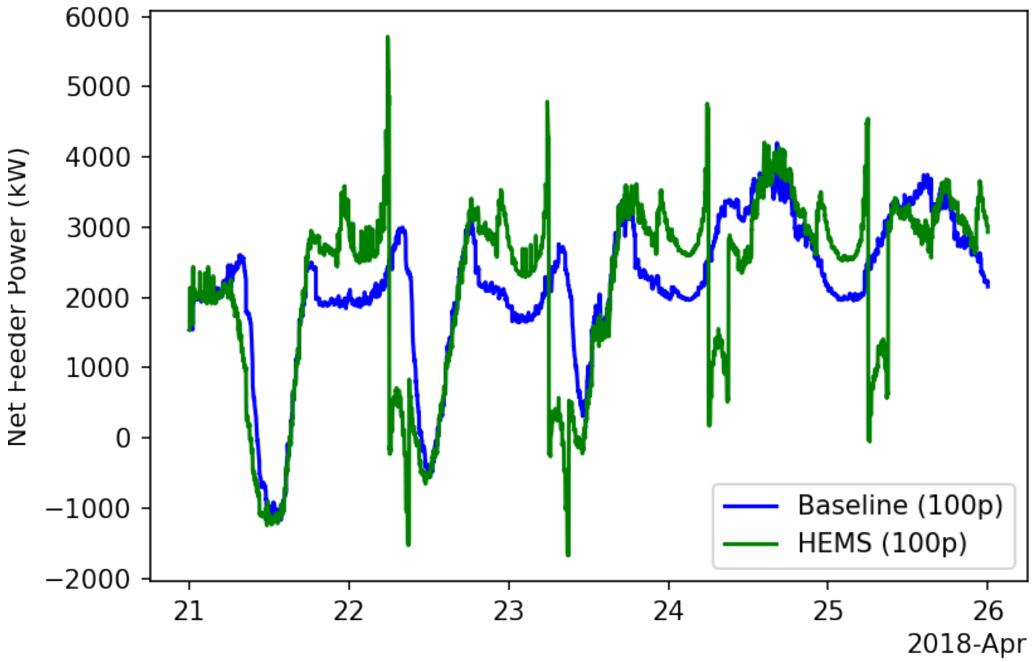

Figure 13. Net power at the feeder head for the baseline and HEMS scenarios with 100% DER penetration.

The HEMS changes the load profile of the home batteries, HVAC, and water heating equipment. Load profiles by end use are shown in Figure 14 for the HEMS scenario with 100% DER penetration in the shoulder season. The battery is charged at night before the morning peak pricing period and is discharged during the peak pricing period (6–9 a.m.). The HVAC and water heating load profiles also reduce loads during the TOU period.

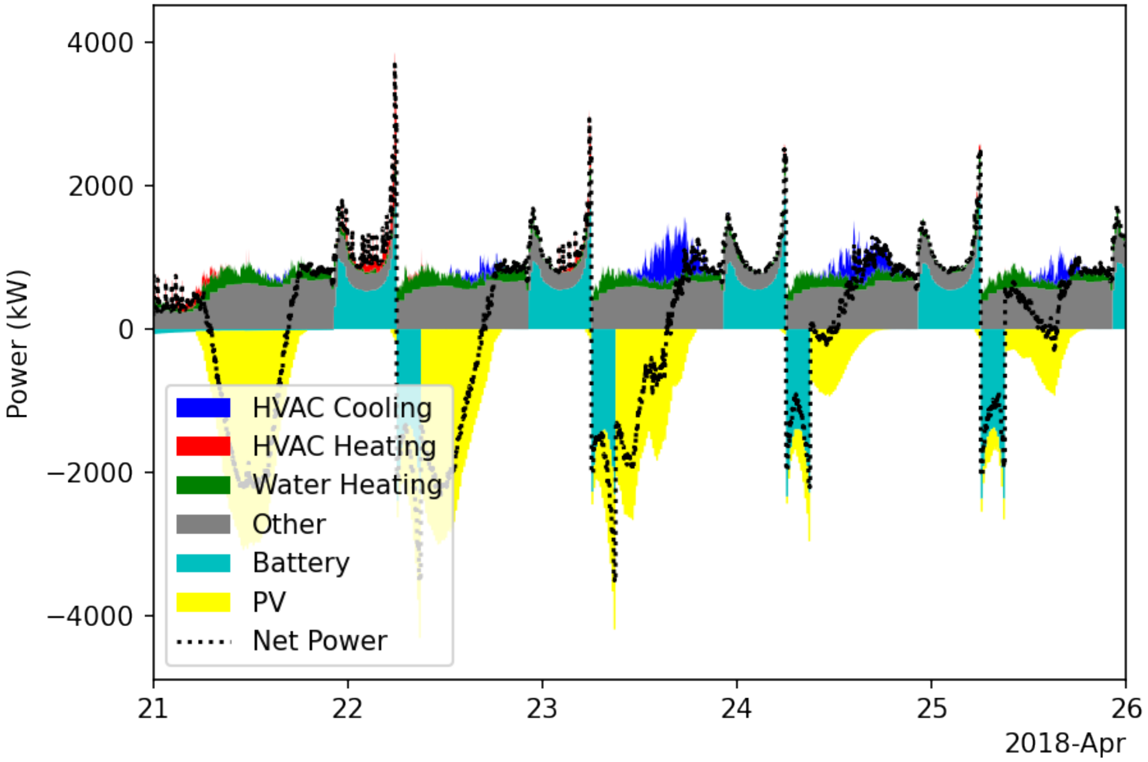

Figure 14. End-use load profiles for the HEMS scenario with 100% DER penetration.

The transactive market scenarios significantly reduce the grid export of the community. Figure 15 shows the net power at the feeder head for all scenarios with 100% DER penetration. The market scenario has no exports back to the feeder as opposed to the other scenarios with 100% DER penetration, thus achieving the goal of the market.

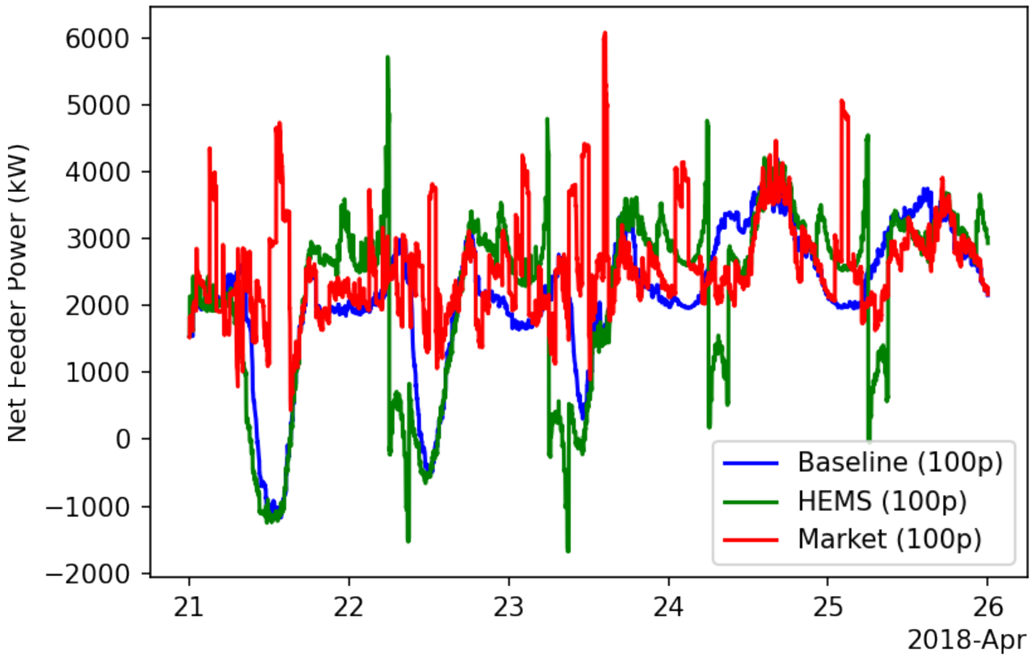

Figure 15. Net power at the feeder head for all scenarios with 100% DER penetration.

Figure 16 shows the end-use load profiles for the market scenario with 100% DER penetration. Multiple loads, including HVAC, water heating, and battery charging, tend to occur when PV generation is high to reduce grid export. There is also more battery cycling and some PV curtailment for some days when necessary.

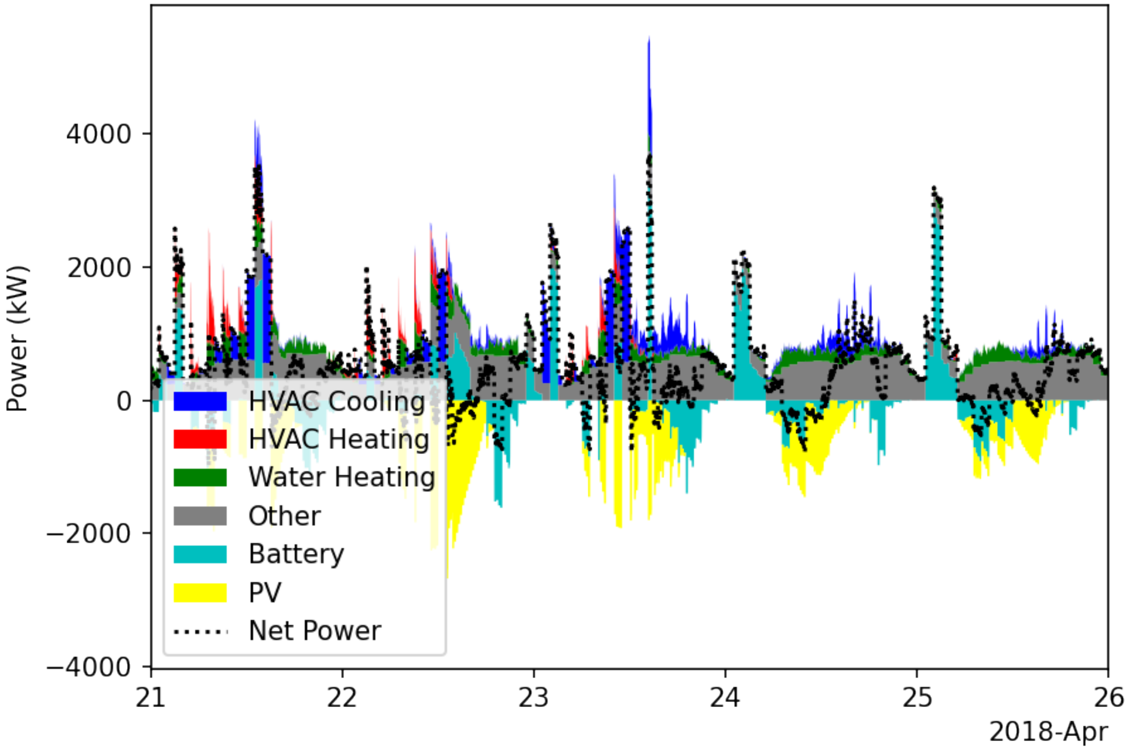

Figure 16. End-use load profiles for the market scenario with 100% DER penetration.

7.1.1 Feeder Metrics

A summary of power metrics for all scenarios is shown in Table 2. All metrics are based on measurements at the feeder head. The BAU scenarios have the most grid import compared to other scenarios, and no grid export. Net energy decreases as DER penetration increases. Compared to the baseline scenarios, the HEMS tends to reduce net energy consumption but increase the maximum import and export.

Table 2. Summary of Power Metrics for All Scenarios

Scenario	Total Import (MWh)	Total Export (MWh)	Total Net Energy (MWh)	Max Import (MW)	Max Export (MW)
Baseline (BAU)	347	0	347	4.4	-
Baseline (100P)	266	-5	261	4.0	1.1
HEMS (BAU)	340	0	340	4.2	-
HEMS (100P)	266	-8	258	5.0	1.6
Market (BAU)	340	0	340	4.8	-
Market (100P)	308	0	308	5.5	-

A summary of voltage metrics for all scenarios is shown in Table 3. Voltage metrics are calculated based on the bus voltages connected to modeled residential loads only. Nearly all voltages remain above 0.95 p.u. in all scenarios. In scenarios with high DER penetration, some voltages exceed 1.05 p.u. The Market scenario with high DER penetration has significantly fewer overvoltage violations than the other high penetration scenarios.

Table 3. Summary of Voltage Metrics for All Scenarios

Scenario	Max V	Min V	Avg V	Percent > 0.95	Percent > 1.05
Baseline (BAU)	1.042	0.923	1.017	99.996	0
Baseline (100P)	1.065	0.950	1.022	100	0.581
HEMS (BAU)	1.042	0.914	1.018	99.997	0
HEMS (100P)	1.090	0.885	1.022	99.994	1.534
Market (BAU)	1.046	0.918	1.018	99.994	0
Market (100P)	1.063	0.888	1.019	99.888	0.043

7.2 Market Analysis

In this section, we provide a detailed look at market operations and demonstrate the drivers for eliminating export at the feeder head. We look at scenarios 3a and 3b and assess market settlement under these two DER penetration scenarios in both the day-ahead and real-time markets.

As shown in Figure 17, in the 3a scenario (BAU), the market always settles at the ceiling. This is due to lower levels of DER and therefore reduced supply bids relative to demand. This trend continues into the real-time market where we do not see any deviation from the day ahead settlement. This is expected behavior for low DER penetration and results in both demand and supply paying (or being compensated at, in the case of supply) the ceiling price. Given that the ceiling was established to achieve equal cost recovery as the prevailing utility tariff, this is essentially a transition to real-time pricing that results in roughly the same cost to the market participants. Additionally, it reflects a real-time pricing version of net metering, as the supply gets remunerated at the current retail price.

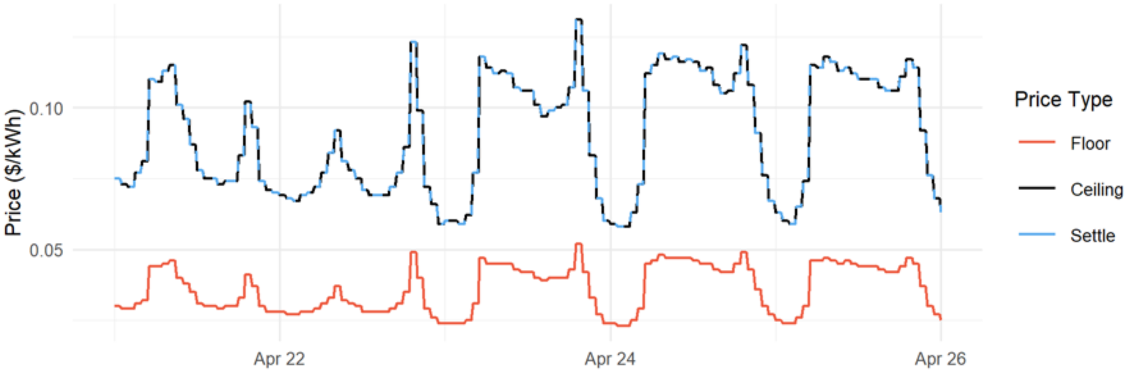

Figure 17. Day-ahead market settlement for scenario 3a (BAU). Ceiling and floor are shown by black and red traces respectively, with settled price shown in dashed blue line (overlaying the ceiling in this case).

Given the straightforward nature of the 3a (BAU) scenario, we turn our attention to the 3b (100P) scenario. As seen in Figure 18, under higher DER penetrations, the day-ahead market settles at the floor during the middle of the day on certain low-load, high-generation days. This is due to large amounts of PV supply bids that are placed at the floor value, exceeding the amount of firm demand that was bid in at the ceiling.

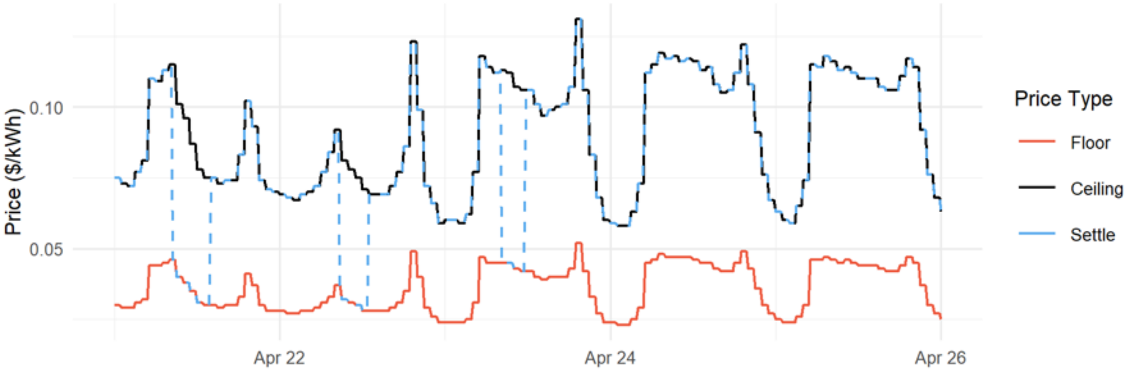

Figure 18. Day-ahead market settlement for scenario 3b (100P). Ceiling and floor are shown by black and red traces respectively, with settled price shown in dashed blue line.

Figure 19 shows market clearing for a single timestep, demonstrating the impact of the high DER penetration. In the right tile of Figure 19, we see that the firm demand—bid at the ceiling—in scenario 3b has been greatly reduced by self-consumption of PV, as compared with the higher amount of firm demand and lower supply from scenario 3a (shown in the left tile). Additionally, significant supply bids have resulted in the demand and supply curves intersecting at the floor (where flexible demand has been bid at the market floor) and thus settlement at that lower price.

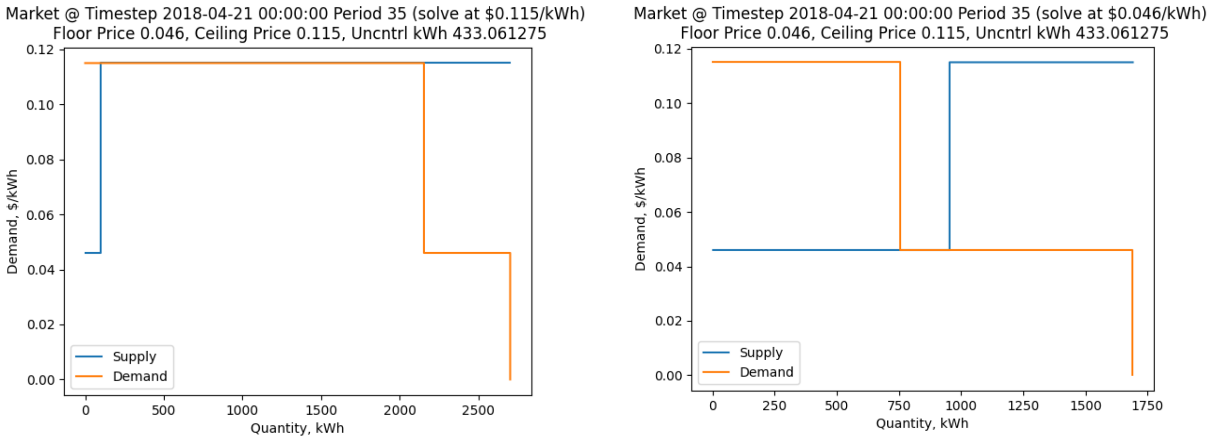

Figure 19. Comparison between market clearing in scenario 3a (left graph) and scenario 3b (right graph) during a single timestep at 9am. The 3a scenario clears at the ceiling, whereas scenario 3b clears at the floor price.

After settlement of the day-ahead pricing, the market transitions into real-time operation. This market runs each hour, yet bids are submitted to the market for the market hour as well as the seven subsequent hours. When the market module receives those bids, it communicates back approved bids for the upcoming hour as well as any forecasted surplus pricing over the following seven hours. A snapshot of this is shown in Figure 20, where we can see the updated real-time forecast during real-time market execution at 8 a.m. on April 22. Given the submitted real-time bids at that point in time, the market is forecasting significant surplus pricing.

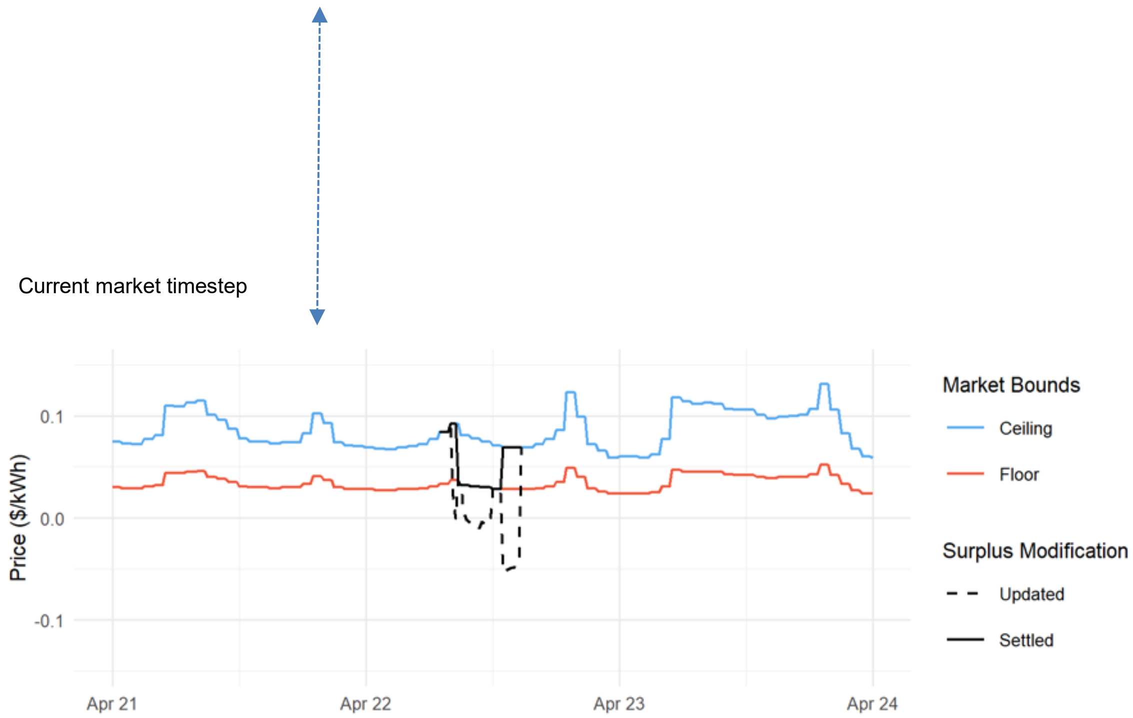

Figure 20. Real-time market operations showing both settled day-ahead pricing (solid black trace) and updated real-time price forecast (dashed black trace) including predicted surplus pricing based on bids received.

It should be noted that these are non-binding bids at that time and much of this surplus pricing will not actually manifest in the settled real-time price because the HEMS are able to pull out generation bids or include additional demand bids in response to this forecast. This can be seen in Figure 21, where the significant forecasted surplus pricing has not manifested in the final settled price. We note that surplus pricing still does take effect in certain hours, as only so much demand and supply can be shifted.

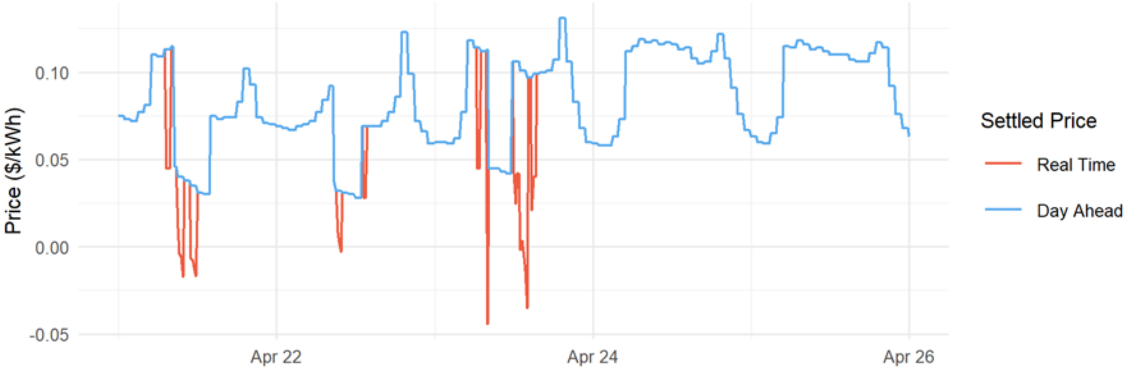

Figure 21. Settled real-time price, overlaid on the settled day-ahead pricing.

The evolution of the market operation described in this section results in sufficient incentives for the buildings to pull generation at appropriate times and accomplishes the goal of net zero export at the feeder head. This is not to say that the market design is 'optimized' or final; rather, it demonstrates that market designs can achieve the goals set out for the project. Specifically, this market has not been tested for 'gaming' opportunities or malicious behavior by participants. Finally, all participants are assumed to have a HEMS that can support bid construction, which is a key element in making this market implementation tractable from a customer engagement perspective.

7.3 House Analysis

Figure 22 shows the house loads, by end use, of one of the houses participating in market for scenario 3b. The house is equipped with a gas furnace, central air conditioner, and gas tank water heater. The house is also equipped with a 6.9-kW PV system and Tesla Powerwall two-battery system. As the air conditioning is a major load in the house, there are spikes in the net power of the house when the air conditioner operates. The PV is curtailed during certain times of the day, especially during April 21, in scenario 3b. However, during times of low PV production on the feeder on April 24 and April 25, the PV is not curtailed.

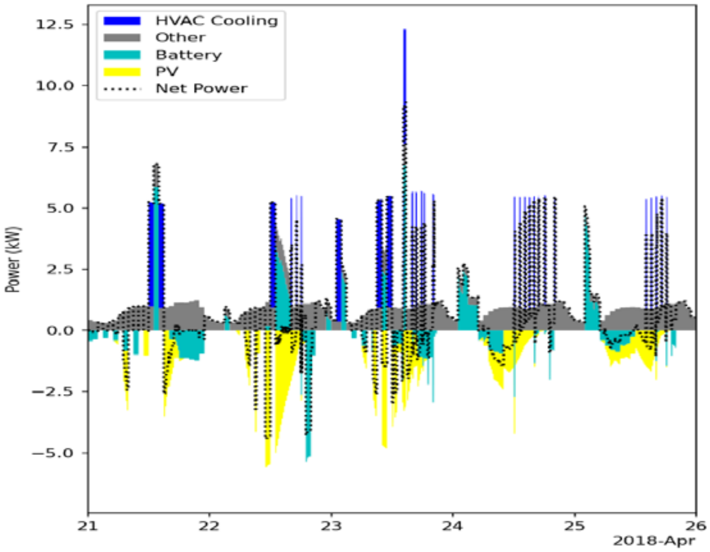

Figure 22. House loads by end use.

Figure 23 shows the comparison of indoor air temperature of the same house between a baseline scenario (1b) and market scenario (3b). The heating and cooling setpoint temperature of the house in the baseline case is maintained within the thermostat dead band around the setpoint. For the market scenario, **foresee** considers a comfort band around the setpoint temperature for providing additional flexibility. There is minor deviation from cooling setpoint temperature in 3b compared to baseline case. This is because **foresee** attempts to maintain the indoor air temperature around the upper comfort band for cooling to minimize the air conditioning energy consumption. However, the indoor temperature is still within the comfort band for cooling.

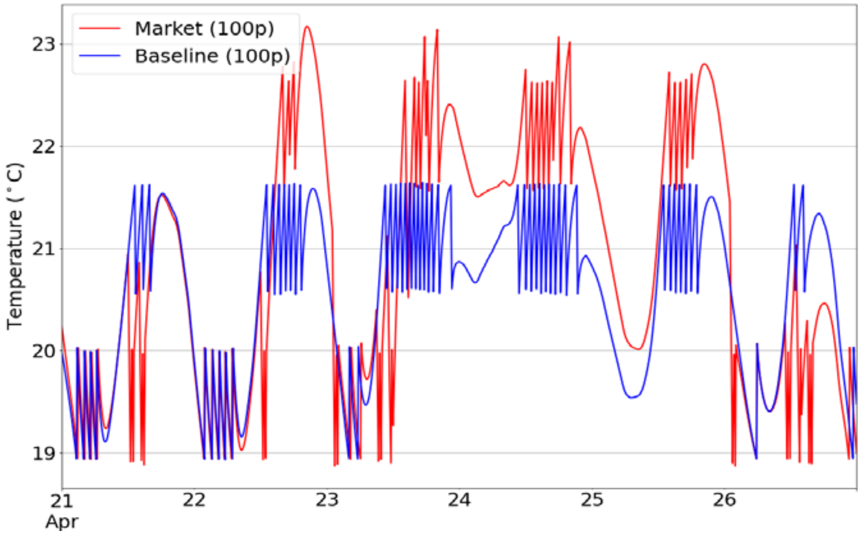

Figure 23. Comparison of indoor air temperature.

The demand and supply bids submitted by **foresee** of the same house in the day-ahead market for a single day, April 24, is shown in Figure 24. The hatching lines in a bid signify that the bid was not accepted in the market. In this house, **foresee** is controlling PV, battery, and air conditioner, and bidding the supply and demand bids in the market. For the day-ahead bids, there are demand bids during the early morning and in the late evening. The high demand bid during hour 2–3 is because of battery charging load in the house. As can be seen the figure, **foresee** submits the flexible bids in the market but those flexible bids were not accepted in the day-ahead market. There are no supply bids submitted in the market because **foresee** expects to self-consume the PV generation in the house.

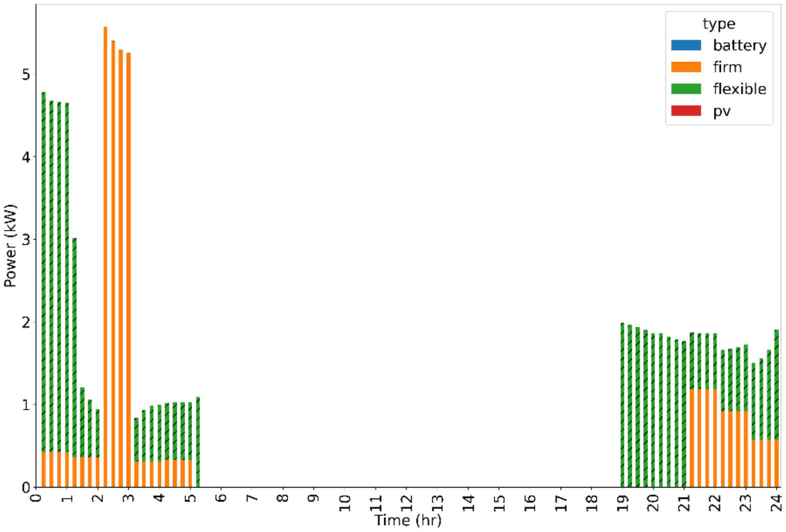

Figure 24. Day-ahead bid for a single day, April 24.

Figure 25 shows the real-time bids submitted by **foresee** in real-time market for the same day, April 24. The hatching line in a bid represents that the bid was not accepted in the real-time market. As the real-time bid formulation considers day-ahead cleared prices for computing the utility cost, there are some differences between the day-ahead and real-time bids. It is also noteworthy that the day-ahead bids are generated with **foresee** optimizing with a 24-hour horizon, and real-time bids are generated with **foresee** optimizing with an eight-hour horizon. There are higher flexible bid quantities in real-time as compared to the day-ahead flexible bids. There is additional flexibility for DER operation in real-time—even though flexible bids in previous hours were not accepted, **foresee** reoptimizes each hour in real-time with updated information such as indoor air temperature. Similarly, PV bids in the real-time market are accepted. As a result, there is net power export to the grid in real-time as shown in Figure 25.

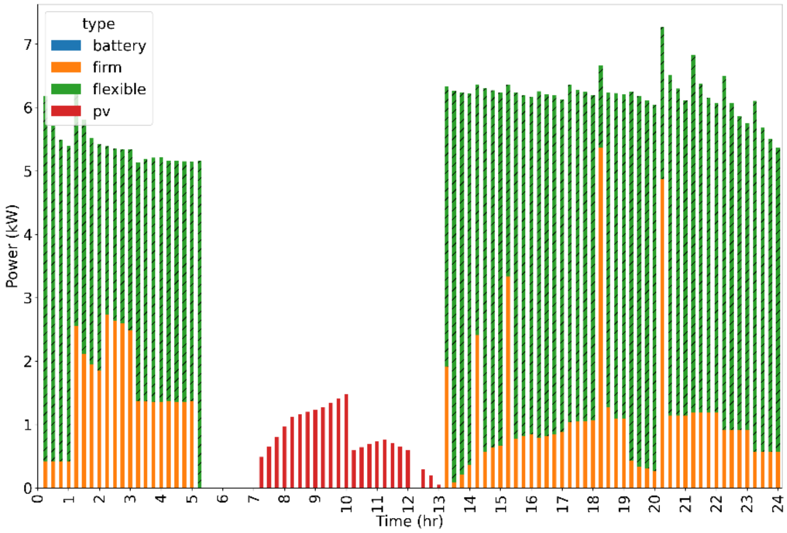

Figure 25. Real-time bid for a single day, April 24.

8 Conclusion

We have provided a detailed design of a transactive energy market and evaluated the market under different scenarios through co-simulation of buildings, DER, and associated HEMS attached to a Pepco distribution feeder. By performing this granular analysis, it has been shown that the goal of a zero-energy export can be achieved on feeders with high DER penetration using the market while providing cost-effective service to the customers and without major disruptions to the grid infrastructure. Although the DERs are coordinated by the market, they are not directly controlled—the customer has control over the building loads and the DERs, enhancing their satisfaction. The addition of bidding capability to the HEMS has made it possible for the customers to participate in the market and maintain the customer's preferences.

In addition to the market design, we have been able to explore real-world implementation pathways using the Energy Web Foundations' blockchain platform and tools. These tools can be leveraged as transactive markets make a transition from simulation to pilot deployments, making those pilot implementations cost effective, reliable, and scalable. We have demonstrated the digital identity management and record keeping EW-DOS in this project and it can be further expanded for future work.

References

D. Cutler, T. Kwasnik, S. Balamurugan, T. Elgindy, S. Swaminathan, J. Maguire, and D. Christensen. 2020. Co-simulation of Transactive Energy Markets: A Framework for Market Testing and Evaluation. Accepted for publication in *International Journal of Electrical Power and Energy Systems*.

X. Jin, K. Baker, D. Christensen, and S. Isley. 2017. Foresee: A user centric home energy management system for energy efficiency and demand response. *Applied Energy* 205, 1583–1595. http://www.sciencedirect.com/science/article/pii/S0306261917311856.

J. Maguire, R. El Kontar, J. Chen, and X. Jin. 2019. "Physics-based White-Box Dwelling Model for Building-to-Grid Integration Studies." Presented at the 2019 Building Performance Analysis Conference, Denver, Colorado, September 27, 2019. https://www.nrel.gov/docs/fy20osti/74946.pdf

M. Morey. 2001."Power Market Auction Design: Rules and Lessons in Market-Based Control for the New Electric Industry." Edison Electric Institute.

P. Munankarmi, X. Jin, F. Ding and C. Zhao. 2020. "Quantification of Load Flexibility in Residential Buildings Using Home Energy Management Systems". 2020 American Control Conference, Denver, Colorado, 1311–1316.

M. Blonsky, J. Maguire, K. McKenna, D. Cutler, S. Balamurugan, X. Jin. "OCHRE: The Object-oriented Controllable High-resolution Residential Energy Model for Dynamic Integration Studies.", Applied Energy, vol. 290, 2021.

U.S. Department of Energy. 2021. "EnergyPlus." Accessed January 7, 2021. https://energyplus.net/.

E. Wilson, C. Christensen, S. Horowitz, J. Robertson, and J. Maguire. 2017. "Energy Efficiency Potential in the U.S. Single-Family Housing Stock." Golden, CO: NREL. https://www.nrel.gov/docs/fy18osti/68670.pdf.

B. Palmintier, D. Krishnamurthy, T. Philip, S. Steve, D. Jeff, and F. Jason. 2017. "Design of the HELICS high-performance transmission-distribution-communication-market co-simulation framework." Presented at the 2017 IEEE Workshop on Modeling and Simulation of Cyber-Physical Energy Systems, Pittsburg, PA